REVIEW ARTICLE | APRIL 25 2025

Nanoscale imaging of biological systems via expansion and super-resolution microscopy

Daria Aristova ; Dominik Kylies ; Mario Del Rosario ; Hannah S. Heil ; Maria Schwerk ; Malte Kuehl ; Milagros N. Wong ; Ricardo Henriques ; Victor G. Puelles

Appl. Phys. Rev. 12, 021311 (2025)
https://doi.org/10.1063/5.0240464

Applied Physics Reviews REVIEW pubs.aip.org/aip/are

Nanoscale imaging of biological systems via expansion and super-resolution microscopy

Cite as: Appl. Phys. Rev. **12**, 021311 (2025); doi: 10.1063/5.0240464
Submitted: 25 September 2024 · Accepted: 1 April 2025 ·
Published Online: 25 April 2025

Daria Aristova,[1,2,3] Dominik Kylies,[4,5] Mario Del Rosario,[1,2,3] Hannah S. Heil,[2,3,6] Maria Schwerk,[4,5] Malte Kuehl,[7,8] Milagros N. Wong,[4,5,7,8] Ricardo Henriques,[1,2,9,a)] and Victor G. Puelles[4,5,7,8,a)]

AFFILIATIONS

[1]Instituto de Tecnologia Química e Biológica António Xavier, Universidade Nova de Lisboa, Oeiras, Portugal
[2]Instituto Gulbenkian de Ciência, Oeiras, Portugal
[3]Gulbenkian Institute for Molecular Medicine, Oeiras, Portugal
[4]III. Department of Medicine, University Medical Center Hamburg-Eppendorf, Hamburg, Germany
[5]Hamburg Center for Kidney Health (HCKH), University Medical Center Hamburg-Eppendorf, Hamburg, Germany
[6]Department of Clinical Sciences Lund, Division of Infection Medicine, Faculty of Medicine, Lund University, Lund, Sweden
[7]Department of Clinical Medicine, Aarhus University, Aarhus, Denmark
[8]Department of Pathology, Aarhus University Hospital, Aarhus, Denmark
[9]UCL Laboratory for Molecular Cell Biology, University College London, London, United Kingdom

[a)]**Authors to whom correspondence should be addressed:** r.henriques@itqb.unl.pt; vgpuelles@clin.au.dk and v.puelles@uke.de

ABSTRACT

Super-resolution microscopy (SRM) has revolutionized life sciences by overcoming the diffraction limit, enabling the visualization of biological structures at the nanoscale. Expansion Microscopy (ExM) has emerged as a powerful and accessible technique that enhances resolution by physically enlarging the specimen. Importantly, the principles of ExM provide a unique foundation for combinations with SRM methods, pushing the boundaries of achievable resolution. This review explores the fundamental principles of ExM and examines its successful integration with various SRM techniques, including fluorescence fluctuation-based SRM, structured illumination microscopy, stimulated emission depletion microscopy, and single-molecule localization microscopy. We discuss the applications, strengths, limitations, and resolutions achieved by these combined approaches, providing a comprehensive guide for researchers to select the most suitable method for their specific scientific needs. Key considerations when combining ExM with SRM include the impact on fluorophores, the requirement for specialized buffers, and the challenges posed by the sensitivity of expanded hydrogels to temperature and hydration. Strategies to address these challenges, such as optimized labeling techniques and gel re-embedding, are discussed in detail. This review aims to assist researchers in navigating the rapidly evolving landscape of ExM and SRM, facilitating the development of tailored imaging pipelines to advance our understanding of biological systems at the nanoscale.

TABLE OF CONTENTS

I. INTRODUCTION

Super-resolution microscopy (SRM) encompasses various methods that overcome the diffraction limit, a physical restriction that limits

the optical resolution of fluorescent microscopes to around 250 nm.[1,2] Subcellular structures such as cellular organelles, cytoskeletal filaments, membrane receptors, and macromolecular complexes are often smaller than the diffraction barrier. Notable examples in different organs include the gap between two neuronal processes, known as the synaptic cleft (approximately 20 nm),[3,4] the endoplasmic reticular lamellae (range: 20–60 nm)[5] and the width of the renal slit diaphragm, the kidney filtering unit (approximately 40 nm).[6] The breakthrough of SRM in surpassing these limitations is therefore of immense importance to achieve a deep understanding of cellular and tissue-based processes in health and disease.[2,7–11] Increasingly, the analysis of cellular ultrastructure also plays an important role in clinical diagnostics.[12,13] Therefore, SRM techniques have become indispensable tools in life sciences, providing key insights into the molecular architecture and dynamics of cells and tissues, as many crucial biological structures and interactions occur at these length scales.[14] Since the introduction of the first SRM methods,[15–21] multiple optical approaches have been developed, including both commercially available solutions and open-source image enhancement algorithms.[22–29] These optical and computational SRM technologies leverage various principles to achieve resolution beyond the diffraction limit, with resolutions reaching as low as 20 nm[26] depending on the method and setup. Furthermore, recent approaches, including Minflux,[30–32] Minsted,[33,34] and RESI[35] have even reported sub-nanometer resolution.

Less than a decade ago, a radically different approach to achieving resolutions beyond the diffraction limit called "Expansion Microscopy" (ExM)[36] was developed. Unlike many other methods to break the diffraction limit, ExM is a tissue processing technique that enhances the resolution of microscopes by physically enlarging biological samples before imaging.[36–40] This eliminates the need for specialized SRM equipment, making ExM relatively simple to implement. One of the key advantages of ExM is its ability to enhance resolution in all three spatial dimensions (3D) and enable thick sample imaging. However, due to the necessity of fixation and separation of biomolecules during the process, ExM is not compatible with live-cell imaging. Since its introduction, ExM has rapidly gained widespread acceptance within the scientific community with an increasing availability of specialized protocols, highlighting its broad applicability as a versatile and valuable tool across various scientific disciplines. Depending on the ExM protocol and the achieved degree of tissue expansion, ExM has been shown to enable resolutions under 70 nm[36,41] using diffraction-limited microscopy systems.

To extend the range of applications, ExM protocols were initially combined with light-sheet[42–45] and conventional confocal microscopes.[36,46] However, the modular nature of ExM as a tissue processing technique makes it compatible with a wide range of microscopy technologies, including SRM [Fig. 1(a)]. In particular, ExM has been successfully integrated with methods such as stimulated emission depletion (STED),[47] single-molecule localization microscopy (SMLM),[48] structured illumination microscopy (SIM),[49] and fluorescence fluctuation (FF)-based SRM algorithms (FF-SRM),[50] demonstrating enhanced resolution and enabling researchers to create novel, modular, and versatile combined SRM pipelines tailored to their specific scientific requirements [Fig. 1(b)]. Other intriguing approaches that leverage combinations of methodologies across disciplines further underscore the potential of integrated techniques, as highlighted in recent studies on advanced imaging and analysis methods.[51–53] However, given the different principles of action and applicability of these SRM methods, individual considerations, including specific strategies for troubleshooting and limitations, must be addressed to achieve optimal results. In this review, we discuss the basic principles of ExM and SRM methods that have been successfully combined with ExM, along with their applications, strengths, limitations, and resolution range, thereby guiding researchers in selecting an appropriate combined method that best suits their scientific needs.

II. EXPANSION MICROSCOPY

ExM is a highly effective specimen processing technique that physically expands samples, enabling resolutions that surpass the diffraction limit of conventional light microscopes.[36] Instead of relying on advanced optics or computational approaches, ExM achieves super-resolution by embedding biological samples in swellable hydrogel polymers. As the hydrogel expands, the biomolecules and their associated fluorescent labels are separated, enabling the visualization of structures below the diffraction limit. This section covers different variations of ExM, their underlying chemistry, and combinations of ExM with SRM techniques. A summary of available ExM protocols is provided in supplementary material Table 1.

A. Terminology

Early studies on tissue clearing, particularly hydrophilic clearing protocols, occasionally observed increases in tissue volume during the clearing process.[54] For example, in 2011, the Scale brain-clearing protocol, which uses substances such as urea and Triton X-100, was observed to cause a 1.25-fold increase in tissue size.[55] Subsequent clearing protocols, including CLARITY[56] and CUBIC,[57] also acknowledged tissue swelling as a treatment by-product. In these investigations, expansion was often seen as a side effect of the clearing process, sometimes discussed as uncontrolled or undesired. Of note, CUBIC-X,[58] an extension of CUBIC, purposefully achieves an approximately 2× linear expansion by using small molecules such as imidazole and antipyrine to induce tissue swelling. Given these findings in the context of the rapidly growing field of ExM, it is important to distinguish between clearing-focused protocols that result in smaller degrees of specimen swelling as a side effect and "true" ExM protocols designed to enable super-resolution through specimen expansion. Thus, "ExM" generally refers to methods that involve embedding a biological specimen into polyelectrolyte hydrogels that are specifically designed and validated to have high degrees of isotropic swelling capabilities while preserving the nanostructure of the biological specimen.

B. Principles

While many protocol variations exist today, the most widely adopted ExM protocols[37] follow a somewhat similar workflow to achieve isotropic specimen expansion while preserving structural information at nanoscopic scales.[38] Notably, in this rapidly evolving field with an increasing number of protocol modifications and variations, the general workflow described here might not fully translate to all protocols available to this date.[59–61] Classically, molecular anchors are covalently attached to biomolecules, facilitating their binding to a swellable hydrogel synthesized across the specimen.[37] Subsequently, the specimen is incubated in a monomer solution [containing sodium acrylate (SA)], allowing the monomers to distribute homogeneously. Next, via free-radical polymerization, a densely cross-linked (via the cross-linker N,N′-methylenebisacrylamide) polyelectrolyte hydrogel (sodium polyacrylate) is formed, resulting in a robust mechanical

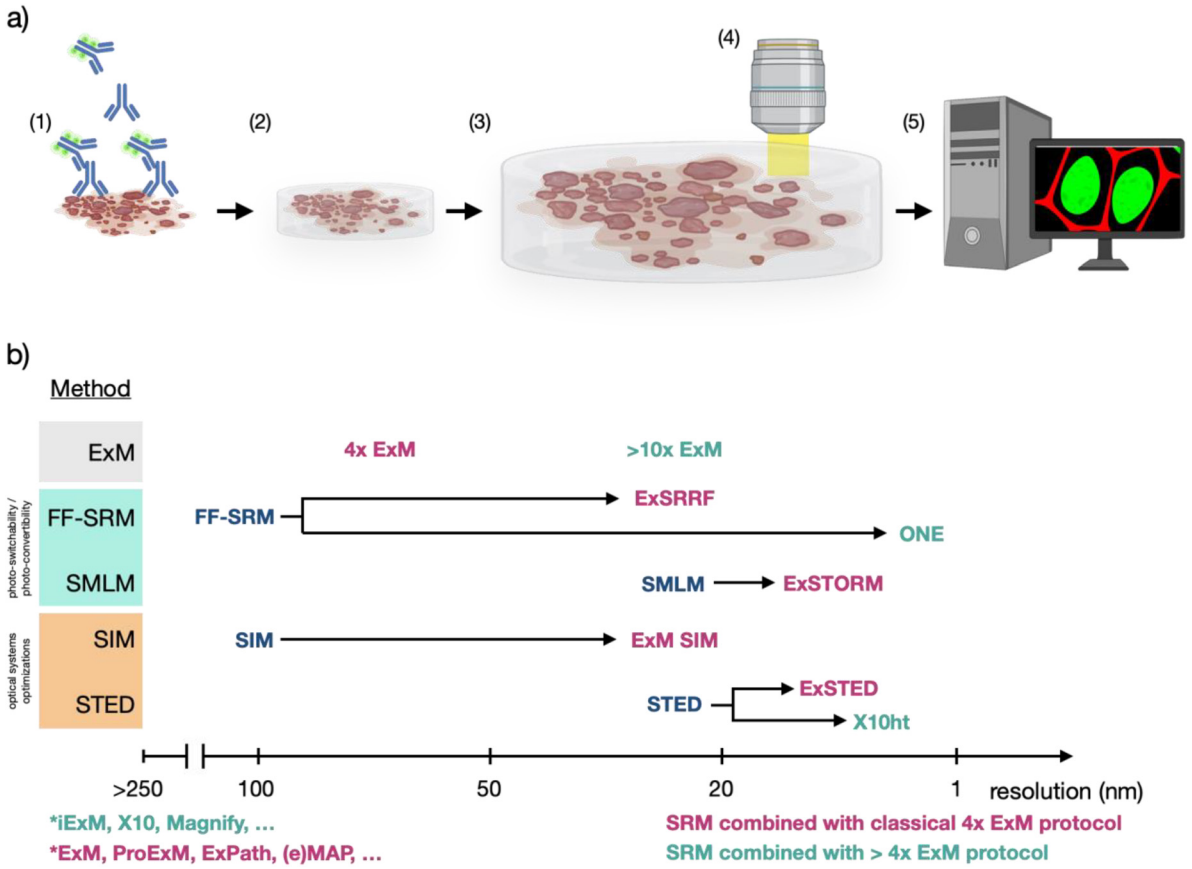

FIG. 1. Overview of combined methods. (a) Graphical overview of the general workflow of combined methods. Biological samples are fluorescently labeled (1), followed by hydrogel embedding (2), and sample expansion (3). The samples are then imaged using different SRM technologies (4), often involving computational processing (5). (b) Resolution range of SRM modalities alone and when combined with ExM protocols. Generally, FF-SRM and SMLM focus on photo-switchability/photo-convertibility while SIM and STED focus on optical systems optimization strategies. While blue text reflects SRM methods without additional expansion. Magenta text reflects SRM modalities combined with a fourfold ExM protocol. The cyan text reflects the combination with a higher-fold ExM protocol.

coupling with the attached biomolecules and fluorescent labels.[36,37] The specimen's mechanical properties are then homogenized through either chemical denaturation via heat and detergent treatment, or enzymatic digestion, depending on the specimen texture and experimental requirements. Finally, immersion in de-ionized water induces isotropic swelling through osmotic force, facilitated by the highly charged nature of the polyelectrolyte mesh.[36]

C. ~4-Fold expansion

The original ExM protocol achieved a 4.5-fold linear expansion with approximately 70 nm lateral resolution.[36] This foundational protocol demonstrated the potential of physically expanding specimens to overcome the diffraction limit of conventional light microscopy. By swelling the hydrogel-embedded sample isotropically, the fluorophores tagging biomolecules are separated, enabling the observation of biological structures below the diffraction limit. In the original fourfold expansion protocol, Chen *et al.* used a polyacrylamide-based hydrogel where acrylamide (AAm) serves as the monomer backbone while N, N′-methylenebisacrylamide crosslinks polymer chains.[36] Biomolecules of interest had to be tagged with a gel-anchorable fluorescent label, which required custom synthesis, posing a hurdle for researchers looking to adopt the method. Additionally, another limitation was its inability to image genetically encoded fluorescent proteins without antibody labeling. However, since its first report, this protocol has undergone several advancements and variations to improve flexibility, applicability, and overall ease of use, aiming to increase accessibility and enhance its performance in specific settings, which are discussed further.

Protein retention ExM (proExM)[37] made ExM more available to the general scientific community by introducing a commercially available cross-linking molecule (Acryloyl-X, AcX) as a novel strategy to link specimen proteins to the hydrogel. Additionally, methacrylic acid N-hydroxy succinimidyl ester (MA-NHS) and glutaraldehyde have also been successfully utilized to bind proteins within the hydrogel.[62] This addressed two of the main drawbacks of the original ExM protocol, namely, the requirement for custom-built gel-anchorable fluorescent labels and the inability to expand and visualize endogenous fluorescent proteins such as green fluorescent protein (GFP), while still achieving a fourfold linear expansion factor. Next, ExPath shares

many similarities to proExM but is optimized for expanding pathology tissue specimens,[63] facilitating the analysis of archival pathology samples (i.e., tumor biopsies) to understand disease-related changes in subcellular tissue-based structures and processes.

In addition to proExM, a new strategy for RNA anchoring to hydrogels termed ExFISH[64] not only provided a new way to anchor RNA molecules but also allowed high-resolution imaging of specific nucleic acid sequences using fluorescence *in situ* hybridization (FISH) in cells and tissues. Importantly, ExFISH also pioneered the strategy of stabilizing expanded specimens by re-embedding them in uncharged gels, preventing shrinkage in environments with higher osmolarity, such as specialized buffers required for FISH[64] and fluorescence *in situ* sequencing[65] in expanded specimens.

D. Beyond 4-fold expansion

For a better resolution using ExM with standard microscopes, advanced ExM protocols have been developed by increasing the expansion factor. These protocols include multiple rounds of hydrogel re-embedding or those achieving higher expansion in a single round. In general, these higher-fold ExM protocols have been reported to attain resolutions in the range of ∼25 nm in combination with conventional diffraction-limited microscopes.

Protocols such as Iterative ExM (iExM),[66] Pan-ExM,[67] and iU-ExM[68] build upon this concept by involving multiple rounds of hydrogel embedding and expansion, achieving up to 20× isotropic expansion. The iExM protocol builds upon the original ExM protocol by introducing a two-step expansion process. After an initial 4.5× expansion, a second swellable polymer mesh is formed within the expanded space, allowing for an additional expansion, leading to a total ∼20× expansion. iExM has been successfully applied to experimental tissue specimens, allowing the visualization of synaptic proteins and dendritic spine architecture in mouse brain circuitry.[66] iU-ExM is built upon the U-ExM protocol[69] to preserve nanoscale ultrastructure in cellular organelles. Inspired by the MAP[39] protocol, iU-ExM optimizes the fixation step using a combination of low concentrations of formaldehyde (FA) and acrylamide and optimizes the homogenization process. Similarly to iExM, iU-ExM involves multiple rounds of hydrogel embedding and expansion, demonstrating its successful application in cellular and tissue contexts.[68] Pan-ExM is a protocol variant optimized for the spatial molecular analysis of cultured cells in their whole-cell ultrastructural context.[67] Pan-ExM involves the incubation of cells in acrylamide (AAm) and formaldehyde (FA) to prevent interprotein crosslinks and a homogenization step using sodium dodecyl sulfate (SDS) and heat to separate neighboring proteins followed by iterative rounds of hydrogel re-embedding to unmask cellular epitopes for subsequent staining. One distinct feature of the Pan-ExM workflow is the application of an NHS ester staining to achieve a pan-protein contrast and provide a general spatial context to specific molecular markers. Another distinctive aspect of pan-ExM is the use of a cleavable amidomethylol bond within the hydrogel's backbone, facilitating subsequent expansion. Delipidation and denaturation, achieved through sodium dodecyl sulfate (SDS) and heat treatment, contribute to the preservation of protein content.

In contrast to protocols involving iterative rounds of expansion, other ExM protocols such as X10-ExM,[70] Tenfold Robust Expansion Microscopy (TREx),[71] and Magnify[72] achieve an approximately tenfold linear expansion in a single round of gel embedding and expansion. X10-ExM achieves high degrees of expansion by introducing an alternative gel chemistry to that of classic ExM protocols like proExM. While proExM relies on a gel composition consisting of sodium acrylate (SA), acrylamide, and N,N′-methylenebisacrylamide, X10 employs a different formulation based on the introduction of N, N-dimethylacrylamide acid (DMAA) to form polymer chains, combined with SA for cross-linking these chains. When exposed to deionized water, this distinctive composition enables the resulting gel to expand over 10× in each dimension. Unlike classical ExM protocols, X10 requires nitrogen degassing during its gel preparation process to eliminate molecular oxygen, which would otherwise inhibit the polymerization reaction. X10 and classical ExM protocols share a common approach for protein retention within the gel, using Acryloyl-X. In the development of TREx, a systematic investigation compared various published gel protocols, pinpointing the optimal balance between expansion factor and gel stability. By introducing a high monomer content alongside a reduced initiator concentration, TREx demonstrated an approximate 10× expansion factor in a single round of expansion while maintaining enhanced mechanical hydrogel stability and achieving a slower and more controlled polymerization rate, which facilitates a homogenous polymerization across the tissue specimen. The systematic analysis also addressed variations in expansion capabilities among different tissue types, proposing a framework for fine-tuning the crosslinker concentration. TREx is compatible with both the expansion of cells and tissues. Magnify[72] is another technology that expands the anchoring capabilities of ExM by incorporating a novel hydrogel formula and anchoring strategy capable of preserving a diverse range of biomolecules. In contrast to classical ExM protocols, which have relied on anchoring molecules specific to particular biomolecule classes, such as proteins or RNA, the introduction of methacrolein represents a major difference. Methacrolein is a small molecule capable of integrating a diverse range of biomolecules, including proteins, nucleic acids, and lipids, all at once into the gel. Methacrolein has been used in fixation protocols and chemically modifies biomolecules similarly to formaldehyde, introducing an isopropenyl functional group that actively participates in the *in situ* polymerization step. Magnify has been applied to cells and tissues.

E. Potential and challenges

ExM has emerged as a widely adopted and established technology, offering extensive validation and boasting a large community of users. Its ease of implementation and robustness make it highly attractive, with applications spanning various fields such as microbiology, clinical pathology, autoimmune disease, cancer biology, neurobiology, degenerative disease, inflammatory disease, cell biology, and many others. As a specimen processing technique, one of the key strengths of ExM lies in its compatibility with a broad array of additional SRM technologies. This versatility allows ExM to be seamlessly integrated into existing microscopy setups, offering the potential to enhance the resolution of both standard microscopes and super-resolution methods. Despite these advantages, ExM presents several challenges and potential limitations that may require careful consideration to be successfully combined with other SRM methods [Fig. 2(a)].

One important consideration in ExM, especially when combined with additional SRM, is the impact on fluorophores and endogenous fluorescent proteins. It has been observed that signal intensity may decrease after ExM, primarily due to fluorophore degradation during

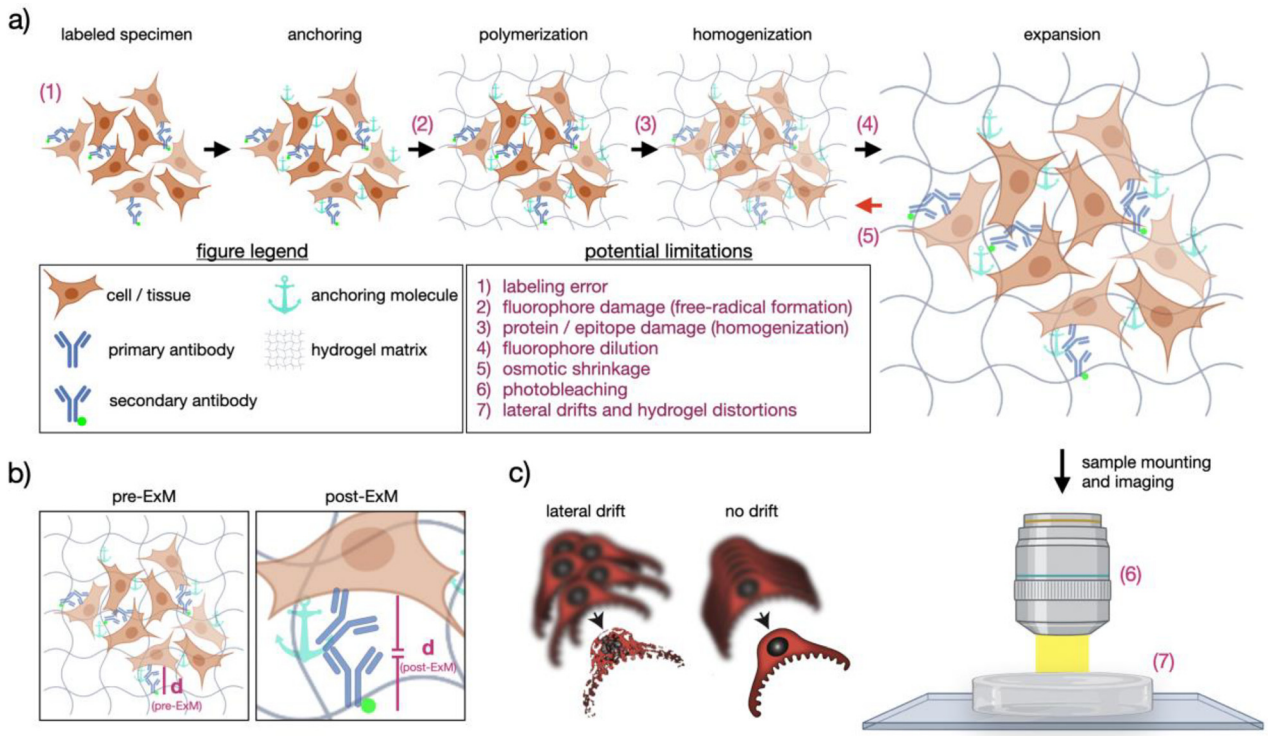

FIG. 2. Expansion workflow and challenges when combining ExM with additional SRM. (a) Graphical overview of the ExM workflow, including critical steps and potential limitations when combining ExM with SRM. After fluorescent labeling, anchoring treatment is performed followed by monomer infusion and polymerization resulting in a sample-hydrogel hybrid. The sample is next homogenized and expanded by incubating the specimen in de-ionized water. The expanded specimens are then mounted and imaged. Potential challenges and limitations in the ExM workflow when combined with other SRMs are highlighted stepwise through numbers (1)–(7). (b) Illustration of linkage error with pre-ExM labeling and fluorophore dilution in non-expanded (pre-ExM) and expanded (post-ExM) samples. Expansion results in increased linkage error as well as a lower number of fluorophores per field of view. (c) Lateral drifts and hydrogel distortions during image acquisition result in diminished image quality and artifacts particularly when combined with methods requiring time-stacked image acquisition. Reproduced with permission from Kylies *et al.*, Nat. Nanotechnol. **18**, 336–342 (2023). Copyright 2023 Authors, licensed under a Creative Commons Attribution 4.0 International License http://creativecommons.org/licenses/by/4.0/.

free-radical polymerization and dilution of fluorescent dyes, particularly in pre-expansion labeling.[37,73,74] For instance, a 4× linear expansion results in a 64× dilution of fluorescent dyes. This dilution effect is more pronounced in ExM protocols that introduce higher degrees of expansion. Additionally, not all dyes are compatible with ExM. For example, cyanine dyes like Alexa Fluor 647, commonly used in SRM methods for their blinking capabilities, often fully degrade during the gelation process.[37,75]

Another factor to consider, especially for endogenous proteins, is degradation due to the digestion process. For example, some fluorescent proteins are prone to degradation when using Proteinase-based digestion. While β barrel-shaped endogenous proteins such as GFP are generally more protease-resistant, other endogenous fluorescent proteins may be more prone to degradation.[37,38,41] Photobleaching is another significant factor in ExM, influenced by degradation, dilution, and the incompatibility of many fluoroprotective mounting media with ExM.[76]

The classic polyacrylamide-based hydrogels, the most widely adopted method for ExM, achieve their maximal expansion when incubated in ddH_2O.[36] The expansion is reversible and can be adjusted by adding more osmolytes to the expansion solution. For example, while incubation in ddH_2O can achieve an approximately 4× expansion factor, incubation in phosphate-buffered saline causes the expanded gel to shrink to a final expansion factor of around 2–3×.[41] The dependence of some SRM methods on specific buffers that modify fluorophore states may, therefore, pose a challenge when combined with ExM.

ExM presents challenges related to the sensitivity of expanded hydrogels to temperature and hydration. Prolonged imaging sessions can lead to dynamic distortions, shrinkage, or micromovements in the expanded samples. Proper mounting of specimens can be challenging, increasing the likelihood of lateral movements during imaging.[77]

Linkage error is an important consideration in ExM, referring to the systematic offset between the fluorescent probe's observed location and the target protein's actual position introduced by the labeling strategy [Fig. 2(b)]. For indirect immunolabeling using primary/secondary antibody complexes, this offset can be as much as 15–20 nm spatially.[78–81] Strategies to reduce linkage error in SRM and ExM include nanobody-based labeling approaches, genetic modifications of the specimen to express fluorescent proteins, self-labeling protein tags, grafting of peptide ligands, or post-expansion labeling in expansion-based methods.[22,48,82–85] Additionally, the degree of fluorescent labeling (DOL) of each tag is crucial to consider. Indirect immunolabeling with secondary antibodies carrying two to five fluorescent markers can

result in a higher fluorescence signal, while smaller tags with DOL close to one yield lower signal levels.

Another factor to consider when combining ExM with other SRM methods is the spatial heterogeneity of expanded gels present at the nanoscale. Conventional polyacrylamide-based hydrogels may exhibit reduced fidelity at scales below 20 nm, which could be a significant factor in their combination with SRM techniques.[86,87]

One more challenge arises when combining Expansion Microscopy (ExM) with super-resolution microscopy (SRM) for 3D imaging. While the transparency and refractive index homogeneity of ExM hydrogels mitigate issues like light scattering, careful consideration must still be given to sample thickness, lens compatibility, and chromatic aberrations, especially at greater imaging depths. Techniques such as STED are well-suited for imaging expanded samples due to their longer working distances, particularly when paired with water immersion objectives.[88,89] These objectives enhance imaging depth and minimize refractive index mismatches with the hydrogel. While effective for thinner samples, SIM may suffer from chromatic aberrations as imaging depth increases.[90] Methods like photoactivated localization microscopy (PALM) and stochastic optical reconstruction microscopy (STORM) are most effective for thin samples (under 10 μm) within a single imaging plane, as they are highly sensitive to optical distortions.[91] To address the challenges posed by thicker expanded samples, lower numerical aperture (NA) water immersion lenses were suggested to improve light penetration and reduce aberrations, though with some loss in resolution.[47,49] Alternatively, cryosectioning expanded tissues can produce thinner sections that are compatible with high-resolution imaging techniques while preserving structural integrity,[92] albeit at the cost of increased sample preparation complexity.

III. COMBINING ExM WITH SRM

Integrating ExM with SRM techniques offers the potential for significant enhancements in resolution. For instance, combining the widely adopted fourfold ExM protocols with open-source super-resolution technologies could yield resolutions comparable to expensive commercial SRM systems, all while retaining the flexibility and efficiency of conventional setups. Moreover, pairing advanced expansion protocols, which achieve higher degrees of expansion, with SRM methods or employing sophisticated optical SRM techniques alongside ExM can push resolution boundaries into the single-digit nanometer range.

The modular nature of these combined methods allows researchers to tailor their SRM pipeline to meet their specific experimental needs, while at the same time using familiar equipment. This facilitates data interpretation and troubleshooting and enables the creation of custom SRM workflows. Furthermore, the addition of ExM can enhance resolution both, laterally and in the z axis, significantly benefiting 3D SRM imaging, regardless of the chosen secondary SRM method.

However, SIM and STED, relying on optical system optimization, and SMLM and FF-SRM, which depend on fluorophore properties like photo-switchability and photo-convertibility, present different challenges when combined with ExM. This section explores the principles and applications of combined ExM and SRM approaches, emphasizing their strengths, challenges, limitations, and potential troubleshooting strategies. Its goal is to offer a comprehensive understanding of these methods, assisting readers in choosing a combined pipeline for their research requirements. The methods are ordered by the level of achieved resolution, and Table I offers an overview of combined ExM and SRM techniques. Supplementary material Fig. 1 further illustrates the challenges and pitfalls of the various combined methods.

A. Fluorescence fluctuation-based super-resolution microscopy

Fluorescence fluctuation-based super-resolution microscopy (FF-SRM) relies on analyzing fluorescence fluctuations over time in a continuous high-speed time-lapse image series, in some aspects similar to the workflow of SMLM. However, FF-SRM generally requires a considerably lower number of frames (typically in the orders of 10–100× less) to render a super-resolution image compared to SMLM, which typically requires the acquisition of several thousands of frames. Additionally, unlike SMLM, which generally requires discrete photoswitching of fluorophores, FF-SRM methods are compatible with both efficient and non-efficient photoswitching fluorophores. This makes the method compatible with a wider range of fluorescent dyes and requires less complex sample preparation.[27,29] In most applications, on its own, FF-SRM achieves a resolution in the range of 50–150 nm depending on the algorithm and microscope used as well as on the particular experimental setup.[26,27,103] FF-SRM methods are compatible with a broad spectrum of microscopes, including epifluorescence, confocal, and total internal reflection fluorescence (TIRF) microscopes and with both fixed and live samples in a multicolor setting.[27,103]

One of the first FF-SRM methods, Super-Resolution Optical Fluctuation imaging (SOFI), was introduced in 2009 and has since been widely adopted by the community.[27,28,104] Among other FF-SRM methods developed,[27,105–111] another widely adopted FF-SRM algorithm, Super-Resolution Radial Fluctuations (SRRF), was introduced in 2016.[29] The SRRF framework stands out for its user-friendliness, resolution, fidelity and modular implementation of computation quality control algorithms.[112] Of note, an updated version called enhanced SRRF (eSRRF) with increased resolution and fidelity, as well as with an added 3D image data analysis feature, was recently introduced.[113]

B. Combining FF-SRM with ExM

FF-SRM algorithms are promising SRM tools for the combination with ExM achieving resolution ranges of 25 nm when combined with a fourfold ExM protocol[50,93] and higher when combined with a higher-fold ExM protocol.[72,94] Both FF-SRM algorithms and ExM protocols are open-access and can be easily implemented across various microscopy setups. They offer flexibility in both sample preparation and data analysis, thus supporting the wider accessibility of higher resolutions in SRM. Unlike some techniques, FF-SRM algorithms do not require specialized fluorophores or buffer systems, allowing for straightforward application with standard immunofluorescence protocols.[27] Many FF-SRM algorithms were originally designed to be compatible with live-cell imaging[103] and therefore do not require high illumination. This makes them well-suited for use with ExM as it reduces photobleaching and laser-induced gel distortions in expanded hydrogels. In addition, their data analysis workflows are often integrated into user-friendly platforms such as FIJI/ImageJ plugins.[29,113]

Despite these advantages, combining FF-SRM algorithms with ExM can still present several challenges that need to be addressed.

TABLE I. Overview of the combined methods.

SRM category	Protocols, references	ExM and SRM methods	Lateral resolution and applied sample type	Advantages and challenges
FF-SRM	ExSRRF[50]	∼4-Fold ExM + SRRF	∼25 nm resolution Clinical and experimental tissues	*Advantages*: 1. No special buffers and fluorophores are required 2. No specialized microscope is required *Challenges and limitations*: 1. Motion artifacts during time-stack image acquisition 2. In general, lower lateral resolution compared to ExM + STED and SMLM
	ExFEAST[93]	∼4-Fold ExM + Airyscan + SRRF	∼25 nm resolution Cells and clinical tissues	
	Magnify[72]	∼10-Fold ExM + SOFI	∼15 nm resolution Human lung organoids	
	ONE[94]	∼10-Fold ExM + SRRF	Resolution not explicitly mentioned but single-digit nanometer resolution implied. Isolated proteins, cells, and experimental tissues	
SIM	ExSIM[49,92,95]	∼4-Fold ExM + SIM	∼25–30 nm resolution Microorganisms,[49] *Drosophila*,[92] and cells[95]	*Advantages*: 1. No special buffers and fluorophores are required 2. High image acquisition speed *Challenges and limitations*: 3. Specialized microscope required 1. Low signal to noise ratio 2. Limited to thin samples, serial cryosectioning for thicker samples required 3. Spherical aberrations 4. Adjustments of the refractive index of oil and water necessary
STED	ExM + STED[96–98] U-ExM + STED[69] ExSTED[47]	∼4-Fold ExM + STED	∼10–20 nm resolution Experimental tissues,[96,98] cells,[47,98] isolated organelles,[69] and microtubules[97]	*Advantages*: 1. High lateral resolution (below 10 nm) 2. No special buffer is required *Challenges and limitations*: 3. STED-compatible fluorophores required 4. Increased photobleaching 5. Low signal-to-noise ratio 6. Signal amplification strategies may increase linkage error
	X10ht-STED[99]	∼10-Fold ExM + STED (cells and vesicles) ∼6-Fold ExM + STED (tissues)	∼6–8 nm resolution Cells, vesicles, and experimental tissues	
SMLM	Ex-SMLM[48] ExSTORM[100] LR-ExSTORM[101]	∼2–3.4-Fold ExM + STORM	∼4–10 nm resolution Microtubules and centrioles,[48] meiotic chromosome[100] Clathrin-coated pits[101] Technical validation of hydrogel expansion fidelity[87]	*Advantages*: 1. High lateral resolution (below 10 nm) *Challenges and limitations*: 1. SMLM-compatible fluorophores required 2. Specific buffers required that may limit the expansion factor 3. Preserving epitopes for post-expansion labeling, which is required to avoid loss of fluorescence 4. Protein digestion step should be adjusted to preserve fluorescent proteins
	Ex-PALM (SExY)[102]	∼5-Fold ExM + PALM	Yeast	

Specifically, issues may arise from artifacts generated by lateral drifts and hydrogel distortions during the time-lapse image acquisition required for FF-SRM algorithms [Fig. 2(c)], or from analytical defects introduced by the algorithms themselves.[112] Furthermore, the additional resolution gained when combining ExM with FF-SRM is generally lower than when combined with other SRM methods such as SMLM and STED. Despite these challenges, the potential of combining FF-SRM with ExM has recently increasingly been recognized and implemented in different scenarios.[50,72,93,94]

Kylies *et al.* developed a novel, modular, and open-source super-resolution pipeline termed expansion-enhanced super-resolution radial fluctuations (ExSRRF)[50] that is optimized for the analysis of clinical and experimental pathology tissue specimens, leveraging the most widely adopted fourfold ExM protocol for pathology specimens[37,63] in combination with the FF-detection algorithm SRRF.[29] ExSRRF achieves a lateral resolution of 25 nm and, when used with conventional widefield microscopes, allows for imaging at various scales, from entire tissue overviews to nanoscale compartments [see Fig. 3(a)]. This facilitates molecular profiling of subcellular structures in archival formalin-fixed paraffin-embedded tissues from complex clinical and experimental specimens, including those from ischemic, degenerative, neoplastic, genetic, and immune-mediated disorders. Furthermore, the authors have shown the potential to combine ExSRRF with customized and open-source image segmentation and analysis algorithms, making it a flexible, robust, scalable, accessible, and adoptable open-source SRM platform.

Another example of combining the FF-based SRM algorithm SRRF with a fourfold ExM protocol is ExFEAST [Expansion fluctuation-enhanced Airyscan technology (FEAST)] developed by Wang *et al.*[93] In contrast to ExSRRF, which focused on the applicability of tissue analysis in a clinical and experimental pathology context, therefore combining ExM and SRRF with LED-based WF microscopes as they represent the most commonly used microscopes in clinical and experimental pathology, ExFEAST applied a similar principle to laser-based confocal microscopes using the Airyscan technology,[25] achieving a lateral resolution of 26 nm. This modular technology was applied to resolve subcellular architecture, such as the cytoskeleton of cells and in human breast cancer samples, where it aided in enhancing the accuracy of counting the average human epidermal growth factor receptor 2 (HER2) copy number for diagnostic purposes.

Klimas *et al.* demonstrated that the combination of SOFI and the novel ExM protocol Magnify achieves an 11-fold expansion factor while retaining nucleic acids, proteins, and lipids without requiring a separate anchoring step.[72] While using only diffraction-limited microscopes, Magnify achieves a lateral resolution of 25 nm. However, when combined with SOFI (Magnify-SOFI) the authors reported a theoretical lateral resolution of around 13 nm under optimal conditions. Among other applications, one example of the improved effective resolution was demonstrated by the visualization of basal bodies in human bronchial basal stem-cell-derived lung organoids that were resolved with Magnify-SOFI but challenging to resolve with Magnify alone [Fig. 3(b)].

The one-step nanoscale expansion (ONE) microscopy method by Shaib *et al.* combines tenfold expansion of the specimen with the fluorescence fluctuation detection algorithm SRRF, enabling the detailed description of cultured cells, viral particles, molecular complexes, and even the structure of single proteins such as antibodies [Fig. 3(c)].[94] Furthermore, while not the main focus of the ONE microscopy manuscript, its applicability was also demonstrated in tissues. In comparison to other methods that combined FF-detection with ExM, ONE microscopy requires a larger number of frames (1000–2000) to generate a reconstruction, needed for the high-order correlations used. In contrast, ExSRRF was shown to use as low as 100 frames for a reconstruction. A lateral resolution of around one nanometer was reported.[94]

Taken together, these studies highlight the potential of combining ExM with FF-SRM to achieve nanoscale resolution across a wide variety of sample types and research questions, ranging from pathology specimens and cells to the structural analysis of proteins at a nanoscale.

C. Structured illumination microscopy

Structured illumination microscopy (SIM) is a commonly used technique for enhancing resolution. For simplicity, we here refer to SIM as an SRM (super-resolution microscopy) technology. While classical SIM is still fundamentally bound by diffraction principles it can still double the resolution of conventional microscopy.[114]

In life sciences, SIM has been applied for live cell and tissue imaging, achieving a resolution in the range of 100–120 nm.[16,17,115–119] The key principle behind SIM is the excitation of the sample with patterned illumination. These patterns interact with the fluorescently labeled sample, creating a moiré effect that encodes high-frequency information into the resulting image.[16] By capturing multiple images with the illumination pattern shifted or rotated and then computationally processing these raw images, it is possible to reconstruct a super-resolved image that effectively doubles the lateral resolution compared to a conventional widefield. There are two main variants of SIM: optical sectioning SIM (here termed OS-SIM) and enhanced-resolution SIM (here termed SR-SIM).[90] OS-SIM uses structured illumination to section the sample optically, removing out-of-focus light and improving contrast,[120,121] while SR-SIM specifically aims to enhance resolution beyond the classical diffraction limit.[122] SR-SIM requires that the emitted light is incoherent from the excitation, which is most commonly used in fluorescence microscopy. SR-SIM works by controlling the excitation in the sample plane, often by generating interference patterns with a periodicity near the diffraction limit that can be readily combined as a postprocessing step.[122] Therefore, image postprocessing is a critical step for SR-SIM.[90,122] SIM is a relatively accessible SRM approach that can be implemented as an upgrade to existing widefield microscope platforms.[123] Advancements in SIM hardware and reconstruction algorithms continue to expand its capabilities, making it an indispensable tool for modern microscopy.[90,123–126] However, SIM is sensitive to sample movement and requires careful alignment of the illumination patterns.[90,127] The computational processing required to reconstruct the final enhanced-resolution image can be time-consuming and will introduce artifacts if not performed correctly.[128]

D. Combining SIM with ExM

SIM technology is well-suited for combination with ExM due to its ease of use and compatibility with multicolor imaging. SIM does not require specialized fluorophores or buffers, making it highly versatile. It offers fast image acquisition compared to other SRM methods, and its data analysis is relatively straightforward.

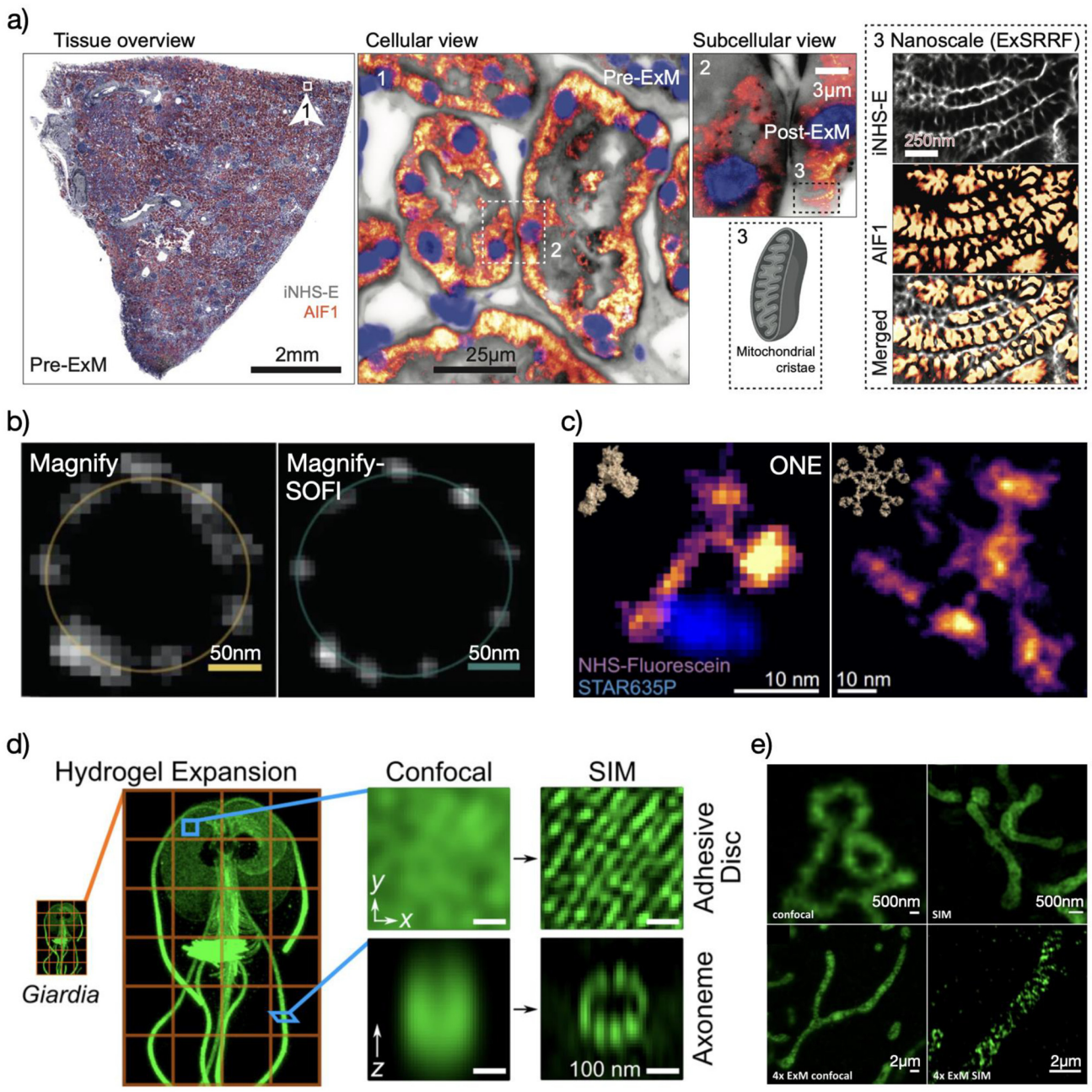

FIG. 3. ExM combined with FF-SRM and SIM. (a) ExSRRF allows nanoscale analysis in clinical and experimental tissues using conventional widefield microscopes by combining a classical fourfold ExM protocol with SRRF, crossing scales from tissue overviews to nanoscale compartments, allowing the visualization of mitochondria and their cristae. (b) The addition of SOFI to the tenfold ExM protocol Magnify further enhances the resolution allowing a clear visualization of basal bodies in human bronchial basal stem-cell-derived lung organoids. (c) The ONE microscopy technology combines a tenfold ExM protocol with SRRF allowing the visualization of nanoscale structures such as antibodies labeled with fluorescent NHS-ester. (d) Combining ExM with SIM enabled the visualization of the adhesive disk and flagellar axonemes in Giardia lamblia. (e) ExM and SIM resolved mitochondria at visually higher resolutions than confocal microscopy, SIM and ExM alone. Reproduced with permission from (a) Kylies *et al.*, Nat. Nanotechnol. **18**, 336–342 (2023). Copyright 2023 Authors, licensed under a Creative Commons Attribution 4.0 International License http://creativecommons.org/licenses/by/4.0/; (b) Klimas *et al.*, Nat. Biotechnol. **41**, 858–869 (2023). Copyright 2023 Authors, licensed under a Creative Commons Attribution 4.0 International License http://creativecommons.org/licenses/by/4.0/; (c) Shaib *et al.*, Nat. Biotechnol. (2024). Copyright 2024 Authors, licensed under a Creative Commons Attribution-NonCommercial-NoDerivatives 4.0 International License http://creativecommons.org/licenses/by-nc-nd/4.0/; (d) Halpern *et al.*, ACS Nano **11**(12), 12677–12686 (2017). Copyright 2017 American Chemical Society; (e) Kunz *et al.*, Front. Cell Dev. Biol. **8**, 617 (2020). Copyright 2020 Authors, licensed under a Creative Commons Attribution License (CC BY) https://creativecommons.org/licenses/by/4.0/.

In general, the resolution range achieved when combining SIM with ExM has been reported to be 25–30 nm.[49,92] Some authors have discussed the potential advantages of combining ExM and SIM (ExM-SIM) over other established SRM techniques, particularly SMLM without ExM, as their resolution ranges are similar.[49] One potential advantage of combining ExM with SIM is the easier implementation of 3D imaging. An advantage is the potentially better resolution and fidelity of ExM-SIM in situations with high labeling density compared to SMLM or FF-SRM methods. While SMLM and FF-SRM perform optimally when imaging sparsely labeled specimens such as thin layers of microtubules or nuclear pores,[129,130] they face challenges with dense samples, leading to artifacts and worse spatial resolution in dense objects.[49,131,132] Additionally, ExM-SIM has a considerably shorter data acquisition time (<1 min/channel) compared to SMLM (>20 min/channel) due to the lower number of images required per image stack. It has also been discussed that ExM-SIM is compatible with a wider range of fluorophores than SMLM, which often requires fluorophores with photoswitching abilities.[26,49] However, challenges remain. Sample preparation and data acquisition parameters should be adjusted to keep photobleaching artifacts to a minimum since expanded specimens are substantially dimmer than unexpanded ones and since 3D SIM requires 15 exposures of the sample per focal plane.[49] Most commercial SIM systems use oil immersion objectives, which can introduce artifacts when imaging deeper into hydrogels due to refractive index mismatches.[49,90]

Halpern *et al.* employed a hybrid imaging approach, termed ExSIM, combining expansion with SIM, achieving a lateral and axial resolution of approximately 30 and 75 nm, respectively.[49] This method was applied to investigate the cytoskeleton of Giardia lamblia, a human pathogen, focusing on the adhesive disk and flagellar axonemes, highlighting ExSIM as a simple and robust modular method for studying biological specimens [Fig. 3(d)]. Due to the limitations mentioned above, the authors applied this method to modestly thick specimens, approximately 8 μm in post-expansion dimensions. While similar to many classical ExM protocols,[37] the ExM protocol applied in this study was modified to contain an increased amount of acrylamide to achieve enhanced mechanical stability while still expanding isotropically, resulting in a final expansion factor of approximately 3.5-fold. This enhanced mechanical stability facilitated the reliable detaching of adherent gel-embedded specimens from their original substrates and overall handling without introducing damage. The authors also introduce a poly-L-lysine strategy for enhanced attachment of hydrogels to cover glass substrates, applied in other workflows.[50]

Cahoon *et al.* combined a fourfold ExM protocol with SIM to enable 3D analysis of the drosophila synaptonemal complex (SC), which has previously proposed a challenge even for advanced SRM methods such as STED.[92] By combining ExM with SIM, the authors took advantage of the resolution increase in all three spatial dimensions that ExM provides, thereby enabling sufficient Z-resolution for 3D analysis of the SC. To overcome the limitations in the working distance of the SIM microscope in large and expanded specimens, Cahoon *et al.* proposed a method of cryosectioning. This involved dehydrating the ExM hydrogels to induce shrinkage, embedding them in tissue freezing media, cryosectioning into 10-μm-thick slices, and re-expanding the sectioned hydrogels. This approach produced samples with a post-expansion thickness of approximately 40 μm, compatible with the SIM microscope's working distance, thereby facilitating 3D analysis using ExM-SIM. The authors reported a lateral resolution of ~25 nm and an axial resolution of ~50–60 nm with the ExM-SIM approach.

Kunz *et al.* combined ExM with SIM to study morphological changes of the mitochondrial cristae as well as the localization of mitochondrial proteins relative to the mitochondrial cristae [Fig. 3(e)].[95] In this study, the authors showcase the utility of a mitochondrial creatine kinase (MtCK) construct linked to a green fluorescent protein (GFP) as a marker for mitochondrial cristae. This MtCK–GFP fusion protein localizes to the space between the outer and inner mitochondrial membranes, making it a reliable marker for cristae. By applying ExM in combination with SIM to mitochondria labeled with this construct, the researchers achieved around 30 nm resolution and were able to visualize morphological changes in cristae.

All these studies demonstrate the potential of combining ExM with structured illumination microscopy (SIM) for addressing complex biological questions. This approach offers significant advantages, such as enhanced resolution and 3D imaging capabilities.

E. Stimulated emission depletion

Stimulated emission depletion (STED) microscopy is a powerful super-resolution imaging technique. Introduced in the 1990s by Hell *et al.*, it became one of the earliest approaches to overcome the diffraction limit of conventional optical microscopes.[15,133] STED microscopy relies on two lasers that form a donut shape. The first laser, known as the depletion laser, switches off the fluorescence of dye molecules at the edges of the excitation laser's focal point. Consequently, only the fluorophores near the center of the depletion beam are allowed to emit fluorescence in their original spectral emission range, reducing the effective size of the detected point spread function (PSF). This process effectively enhances the resolution of the microscope. By carefully controlling the intensity and shape of the depletion laser, state-of-the-art STED microscopes have been shown to achieve lateral resolutions in the range of 20–30 nm.[15,133–135]

STED microscopy has been widely adopted in various fields of biology, from cell biology to neuroscience, enabling researchers to visualize intricate cellular structures, track the dynamics of proteins and organelles, and study the organization and function of biological systems with unprecedented detail.[136,137] Examples of the successful application of STED include the study of synaptic structure and function, as well as the investigation of membrane-associated proteins and their interactions. Additionally, STED has also been applied for *in vivo* imaging.[138–141] Key advantages of STED microscopy include its high spatial resolution and compatibility with 3D image acquisition. Limitations and challenges of STED microscopy include the requirement of specialized and expensive equipment, including a high-power pulsed laser for the depletion beam and complex optical setups.[142] Additionally, the high-intensity depletion laser can photodamage the sample.[143] Despite these challenges, STED microscopy continues to be a valuable tool in modern biological imaging techniques' arsenal, helping researchers achieve a deeper understanding of the complex processes in cells and tissues.

F. Combining STED with ExM

STED microscopy generally provides higher spatial resolution than FF-SRM and SIM, unlike SMLM, does not require special buffers

and eliminates out-of-focus light with its confocal setup. Combinations of ExM and STED have been reported to achieve lateral resolutions below 10 nm.[47,99] However, fluorophore degradation, dilution, and the lack of photoprotective mounting media can interfere with STED imaging when combined with ExM. Therefore, the key challenges are increasing and retaining fluorescent signals in expanded samples.

Unnersjö-Jess *et al.* demonstrated the applicability of a combination of the ca. Fivefold expansion protocol MAP and STED in intact tissue specimens.[96] Through a combination of ExM and STED, the authors were successfully able to resolve two proteins of the renal slit diaphragm simultaneously at resolutions of below 20 nm, highlighting the robustness and versatility of this combined approach in tissues [Fig. 4(a)].

Gao *et al.* applied a combination of a fourfold ExM with STED to resolve the cytoskeleton of cells at high spatial resolution[47] [Fig. 4(b)]. To overcome the limitations of low signal intensity after specimen expansion, a combined and optimized labeling method to maximize epitope coverage was introduced. This involved the expression of α-tubulin–GFP in combination with the use of antibodies against GFP, α-tubulin, and β-tubulin. This approach resulted in approximately a fourfold increase in fluorescence signal for microtubule labeling after gel expansion. In order to achieve better axial resolution, the authors first, used the oil immersion lens close to the surface ($<5\ \mu$m). In this configuration, they achieved an isotropic resolution of 45 ± 4 nm. After overcoming the limitations of mismatched refractive indices between the hydrogel and objective immersion oil, the authors employed two strategies: the first strategy involved the use of a 1.2 NA 60× water objective, which slightly reduced the isotropic resolution to 70 nm but allowed for the complete resolution of the microtubule network. The second strategy involved immersing the sample in a sucrose solution to match the refractive indices of the hydrogel and oil, though this caused the shrinking of the gel reducing the expansion factor by approximately 10%. Ultimately, the resolution achieved was similar for both approaches. Interestingly, it was reported that the use of sucrose was associated with a lower rate of photobleaching. The lateral resolution in this protocol was reported to be below 10 nm and 50–70 nm in the z axis. Limitations to this approach discussed by the authors include photobleaching, and long image acquisition times, especially for the 3D image acquisition of large expanded volumes.[47]

Another attempt to combine ExM with STED was performed to reveal the molecular architecture of centrioles, by using the protocol for preserving ultracellular structure (U-ExM).[69] The authors used the adaptive-illumination scan technique DyMIN (Dynamic Intensity Minimum), which uses reduced light dose, decreasing photobleaching. For labeling, immunostaining with antibodies conjugated to STAR

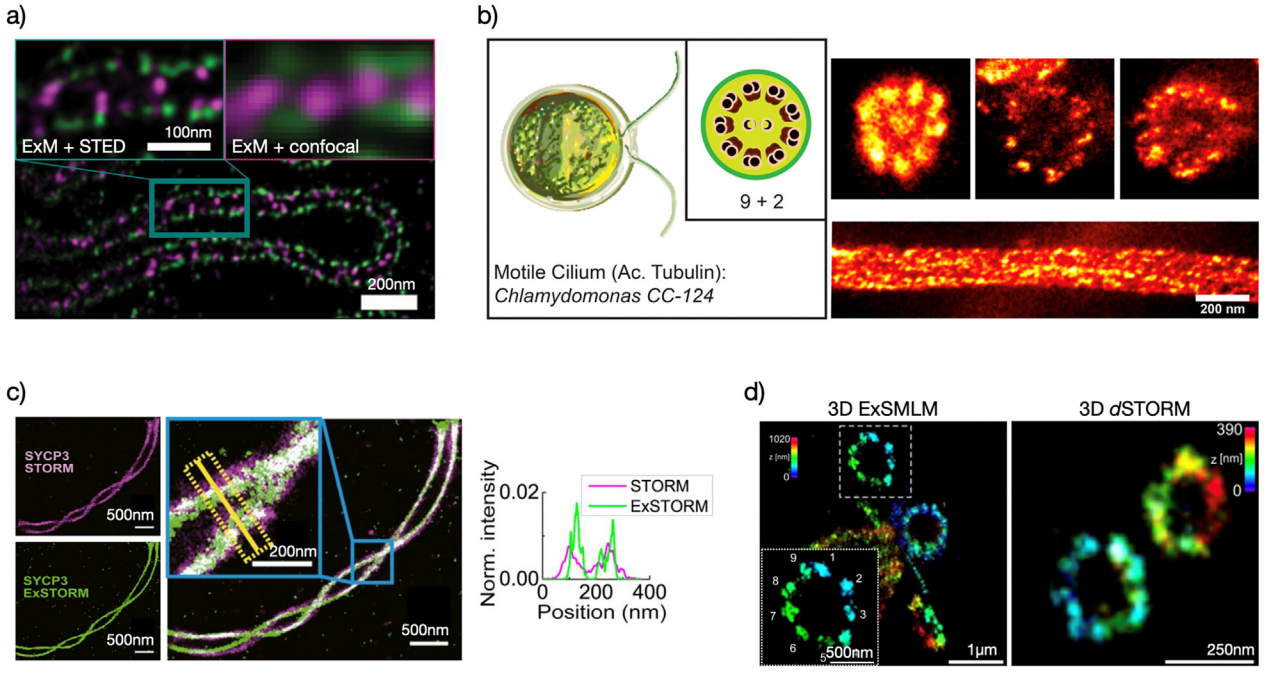

FIG. 4. ExM combined with STED and SMLM. (a) Application of combined ExM and STED in kidney tissues. The combination of ExM and STED visually achieved higher resolutions than the combination of ExM and confocal and enabled the localization of single podocin and nephrin molecules in the filtration slit. (b) ExSTED visualizes cilia in mammalian epithelial MDCK cells. Schematic of motile cilia and cross-sectional and longitudinal views of motile cilia resolved with ExSTED. (c) Comparative analysis of the meiotic chromosome resolved with STORM and ExSTORM revealed significantly higher resolutions for ExSTORM images as shown by sharper peak distributions in the intensity line profiles. (d) Centrioles resolved by Ex-SMLM. 3D dSTORM of expanded Chlamydomonas centrioles reveals the ninefold symmetry at higher resolution and fidelity compared to conventional dSTORM without expansion. Reproduced from (a) Unnersjö-Jess *et al.*, Kidney Int. **93**(4), 1008–1013 (2018). Copyright 2018 Authors, licensed under a Creative Commons CC-BY-NC-ND license https://creativecommons.org/licenses/by-nc-nd/4.0/; (b) Gao *et al.*, ACS Nano **12**(5), 4178–4185 (2018). Copyright 2018 Authors, licensed under a Creative Commons CC-BY license https://creativecommons.org/licenses/by/4.0/; (c) Xu *et al.*, Proc. Natl. Acad. Sci. U. S. A. **116**(37), 18423–18428 (2019). Copyright (2019) Authors, licensed under National Academy of Sciences https://www.pnas.org/pb-assets/authors/authorlicense-1633461587717.pdf; (d) Zwettler *et al.*, Nat. Commun. **11**, 3388 (2020). Copyright 2020 Authors, licensed under a Creative Commons Attribution 4.0 International License https://creativecommons.org/licenses/by/4.0/.

Red/STAR 580 was used. These dyes are known for their brightness and photostability. Combining these properties, U-ExM coupled with STED imaging demonstrated the chirality of the centriole.

Li *et al.* developed an enhanced labeling strategy to facilitate the combination of ExM and STED.[98] Here, the authors re-label the sample after expansion using biotin–streptavidin interaction. Initially, the protein of interest was labeled with a biotinylated primary antibody and a fluorescently labeled secondary antibody. After expansion, fluorescently labeled streptavidin was added to the sample, increasing the signal brightness, and thereby facilitating the combination of ExM and STED.

The necessity to implement enhanced labeling strategies is a known requirement. For example, a labeling strategy uses biotin–avidin signal amplification,[97] which exploits the tetrameric structure of avidin to boost signal strength. Standard immunostaining was performed using biotinylated secondary antibodies and streptavidin conjugated with AF488. After expansion, the sample was labeled again with secondary antibodies conjugated with both biotin and AF488. Using biotin as a linker for dye-conjugated streptavidin, this strategy boosted the number of fluorophores attached to each antibody targeting tubulin, thereby increasing the fluorescent signal sufficiently to use the highest depletion intensity in STED. Two signal amplification cycles were needed to achieve sufficient signal for 100% depletion intensity, resulting in a resolution better than 9 nm. However, the linkage error increased with each signal amplification cycle, reaching 12 nm. For this reason, AviTag was used to directly biotinylate the target protein. Despite this, depletion intensity greater than 50% could not be achieved even after two signal amplification cycles.

Saal *et al.* combined STED with a 10× ExM protocol.[99] In order to overcome limitations of reduced fluorescence intensity in expanded specimens, strategies to achieve optimized retention of fluorescence intensity, epitope preservation and label retention were implemented. A modified digestion step used heat homogenization at 135 °C under alkaline conditions as opposed to a commonly used proteinase-based digestion, as well as an optimized anchoring through applying an increased concentration of the anchoring agent Acryloyl-X. This strategy allowed an up to 11-fold unidimensional expansion under optimal conditions, and the use of nanobodies as labeling agents by preventing their washout, enabling multicolor STED imaging at lateral resolutions below 10 nm. Despite these optimizations, however, the expanded samples were still significantly dimmer, which can partially be attributed to the 1000-fold dilution of fluorophores in the expanded volume. Saal *et al.* devised several methods for post-expansion signal amplification to amplify signal intensities. The most effective signal amplification, up to sevenfold, was achieved using primary nanobodies carrying the ALFA-tag, detected by an anti-ALFA nanobody (NbALFA) fused to a FLAG-tag spaghetti monster (SpaMo36), an engineered GFP with seven FLAG-tags. These tags were further detected by anti-FLAG antibodies followed by secondary antibodies. The resolution achieved by X10ht-STED is suitable for investigating small structures such as protein complexes. However, amplification systems can introduce localization errors, which depend on the type, number, and timing (pre/post-expansion) of labeling tools (ie. nanobodies and antibodies). Consequently, the effective resolution varies based on the specific labeling method.

STED has also successfully been applied as a technical method to determine the homogeneity of sample expansion.[43,69,74]

G. Single-molecule localization microscopy

Single-molecule localization microscopy (SMLM) refers to SRM methodologies that achieve nanoscale resolution by pinpointing the center of emission of a single fluorescent molecule. This is achieved by inducing fluorophores to switch between transient "on" and "off" states, a process often termed "blinking." These blinking events are captured in continuous time-lapse image acquisition of typically several thousand individual frames. The subsequent computational detection of the positions of blinking molecules leads to a high-resolution image reconstruction of their position in space. Because within each frame, only a small fraction of the fluorescent dyes is in the "on" state, the likelihood of two fluorophores spatio-temporally overlapping their transient emissions is very low. Therefore, each signal detected can be interpreted as belonging to an individual molecule even when imaged using a diffraction-limited microscope. Under optimal conditions, SMLM can achieve very high lateral resolutions in the range of as low as 10–30 nm. However, SMLM often requires specialized fluorophores that can be converted into a blinking state through the implementation of tailored imaging buffers, and an optimized labeling density to minimize the spatial overlap of blinking events, which hinders the detection of individual molecules.[26]

Some of the earliest implementations of single-molecule localization techniques include the introduction of photoactivated localization microscopy (PALM) in 2006 by Betzig *et al.*[18] Generally, PALM relies on using photoactivatable or photo-convertible fluorescent proteins that can be induced to switch into a spectral channel, imaged one at a time, localized, and then bleached.[144–147] Stochastic optical reconstruction microscopy (STORM) leverages similar principles as PALM. However, instead of using fluorescent proteins, in its initial implementation, STORM used pairs of Cy3–Cy5 dyes to achieve switchable behavior.[19] A STORM variant dubbed direct stochastic optical reconstruction microscopy (dSTORM) furthered the concept that conventional photoswitchable fluorescent dyes such as Cy5 and Alexa Fluor 647 can also be reversibly cycled between fluorescent states without needing a paired dye such as Cy3.[21] Despite their differences, STORM, dSTORM, and PALM share the fundamental principle of manipulating the fluorescence of individual molecules to bypass the diffraction limit, enabling researchers to visualize cellular structures and processes with unprecedented detail. The choice of technique often depends on the specific requirements of the research question and the available instrumentation and expertise.

H. Combining SMLM with ExM

Combining SMLM with ExM introduces several relevant challenges that need to be addressed to enable optimal functionality. For example, the application of blinking buffers that are required in many SMLM methods can interfere with the expansion factor of the hydrogels that achieve maximal expansion factors through incubation in deionized water and can shrink when in contact with solutions with higher osmolarity. Another challenge is the need for specialized fluorophores that can be converted into a blinking state in a hydrogel environment and survive the expansion process. Despite these challenges, efforts have been made to combine ExM with STORM and PALM.

Xu *et al.* combined ExM with STORM to study the molecular organization of the mammalian meiotic chromosome axis,[100] achieving resolutions in the range of 10–20 nm and thereby a threefold improvement in higher resolutions in their combined approach

compared to STORM alone [Fig. 4(c)]. Additionally, the authors confirmed the fidelity of this combined approach using the vector field method to measure distortion introduced by hydrogel expansion, revealing only minor spatial distortions in the range of 1%–2% at different scales. To prevent gel shrinkage caused by ionic switching buffers, the authors expanded the gel into a low ionic strength buffer, achieving a reduced but effective expansion of approximately threefold. Therefore, the authors demonstrate the possibility of combining ExM with STORM to increase the resolution.[100]

Zwettler *et al.* successfully combined ExM with STORM by employing a different approach to use blinking buffers in conjunction with expanded hydrogels.[48] To prevent interactions between ions in the photoswitching buffer and ionic side groups of the gel that cause gel shrinkage, the authors re-embed the expanded charged hydrogel into an uncharged polyacrylamide gel. This stabilized the expanded hydrogel, albeit at the cost of a slight reduction in the gel expansion factor of approximately 20%.[48,64] Overall, this strategy resulted in an effective increase in spatial resolution as compared to STORM alone [Fig. 4(d)]. In addition, Zwettler *et al.* also tested an alternative strategy to enable the combination of ExM with STORM by using a spontaneously blinking Si-rhodamine dye (HMSiR) to avoid the need for a photoswitching buffer and subsequent re-embedding of the gel, thus in theory circumventing hydrogel shrinkage. However, the pH of the double-de-ionized water of $\leq$7.0 adversely affected the blinking characteristics of HMSiR, rendering it insufficient for SMLM. While the addition of PBS to the expanded hydrogel mitigated this limitation, it resulted in a considerably lower expansion factor of only around twofold, again limiting the spatial resolution of the hydrogel. It should be mentioned that the authors used post-labeling ExM to reduce linkage error and increase resolution. In this article, the authors hypothesized that after 4$\times$ expansion, the immunolabeling linkage error of 17.5 nm (due to primary and secondary antibodies) would reduce to 4.4 nm, the size of a tubulin monomer. Thus, combining single-molecule localization microscopy (SMLM) with post-expansion labeling could reduce the linkage error by the expansion factor, enabling fluorescence imaging with molecular resolution and re-embedding the gel allows for performing STORM on the expanded sample. The authors successfully applied this approach to visualize microtubules and centrioles using organic fluorophores, achieving minimal linkage error.[48]

To overcome the problem of loss of fluorescence during expansion, Shi *et al.* created a trifunctional anchor, a molecule with one arm for binding to antibodies or SNAP and CLIP tags, a second arm with methacrylamide for anchoring into the gel, and a third arm with biotin or digoxigenin for conjugation to an organic dye after expansion.[101] This method preserved up to six times higher fluorescence signal compared to proExM. The high level of label retention with trifunctional anchors, along with high labeling efficiency, allowed the authors to achieve 34 nm resolution with SIM and up to 4 nm effective localization precision with STORM and visualize in high detail clathrin-coated pits. The authors examined commonly used photoswitchable dyes, such as Cy5, Cy5.5, and AF647, and no loss of brightness or photoswitching kinetics was observed. However, the necessity of using a photoswitching buffer caused a lower expansion factor of 3–3.3. Nevertheless, the authors demonstrated that LR-ExSTORM achieved higher resolution and revealed far more details than STORM alone.

Vojnovic *et al.* recently established a specialized method for the super-resolved analysis of yeast termed "Single-molecule and Expansion microscopy in fission Yeast" (SExY), combining ExM with the SMLM technology Photoactivated Localization Microscopy (PALM).[102] The combination of ExM and PALM was chosen for its use of fluorescent proteins as labeling agents, allowing for high labeling efficiency and specificity while eliminating the need for a photoswitching buffer. However, one challenge of this approach of combining PALM with ExM was the degradation of fluorescent proteins during the overall expansion process. To overcome these challenges, the authors implemented an optimized version of the proExM protocol, significantly enhancing the retention of fluorescent signal from 22% to around 50% while enabling a fivefold unidimensional expansion. This was achieved by sequential incubation in monomer solutions: starting with incubating the specimen in a monomer solution that did not contain the initiator Ammonium Persulfate (APS), followed by adding an APS-activated monomer solution. The sample was imaged at 10–80 μm depth.

In addition to biological applications, a combination of ExM with STORM was also used as a validation tool to measure the single-molecule distortions resulting from hydrogel embedding itself. The authors used DNA origami technology and STORM to evaluate structural preservation in hydrogels with different compositions: polyacrylamide, the most commonly used material in ExM, and tetra-gel, a hydrogel that does not rely on free-radical chain-growth polymerization. The results showed that tetra-gel is more accurate and effective at preserving molecular structures during the expansion process.[87]

IV. DISCUSSION AND OUTLOOK

ExM is an easy and widely used method for achieving nanoscale imaging using conventional microscopes. To further enhance achievable resolution, researchers worldwide are exploring the potential of combining ExM with additional SRM techniques. Numerous papers have been published on attempts to combine ExM with SIM, STED, SMLM, and FF-based SR techniques so far. As it was seen, the successful integration of ExM with SRM is not without challenges. One major consideration is the impact on fluorophores and endogenous fluorescent proteins, which can suffer from degradation during the gelation process, partial loss of the protein of interest and fluorophores due to insufficient anchoring to the gel, and dilution of fluorescent signal due to the physical expansion of the specimen. This issue is particularly pronounced in higher-fold expansion protocols and can limit the achievable resolution. Rapid photobleaching of fluorophores and poorer photophysics of organic dyes in the hydrogel's aqueous environment also occur, while many SRM techniques rely on bright and photostable fluorophores. Moreover, linkage errors become a significant challenge as resolution increases. Consequently, improving labeling strategies is crucial. Another challenge arises from the sensitivity of expanded hydrogels to specific buffer conditions required by SRM methods, including SMLM, which can cause the gels to shrink and compromise the expansion factor.

To address these limitations, various strategies have been developed. For example, optimized labeling techniques such as post-expansion labeling and using smaller probes like nanobodies can help minimize linkage errors and improve signal retention. Moreover, different signal amplification approaches were explored to enhance the fluorescence signal by maximizing the fluorophores associated with the molecule of interest.[97,99] Finally, to decrease linkage error and preserve fluorescence different tri- and tetrafunctional anchor probes were developed.[75,101,148–151] Re-embedding expanded gels in

uncharged hydrogels has also been employed to stabilize the samples in the presence of SRM buffers. Additionally, novel gel chemistries and digestion methods have been explored to enhance the mechanical stability and fluorophore compatibility of expanded specimens.

Despite these challenges, the combination of ExM with SRM has already demonstrated its potential to revolutionize our understanding of biological systems at the nanoscale. From resolving the molecular organization of the mammalian meiotic chromosome axis[100] to visualizing the cytoskeletal ultrastructure of cells[48,97] and tissues,[50,72,93,99] these hybrid imaging approaches provide unprecedented access to the intricate details of life. As the field continues to evolve, further advancements in labeling strategies, gel compositions, and imaging technologies are expected to enhance the performance and applicability of ExM-SRM pipelines. Developing novel probes, such as trifunctional anchors and self-labeling protein tags, holds promise for improving signal retention and reducing linkage errors.

Moreover, exploring alternative SRM techniques, such as DNA-PAINT[152,153] and MINFLUX[154] in conjunction with ExM may open up new avenues for achieving even higher resolutions and multiplexing capabilities. Combining DNA-PAINT with ExM presents specific challenges due to the physical properties of DNA and the requirements of each technique. DNA-PAINT relies on DNA hybridization, which requires the presence of metal ions in the solution to stabilize the DNA duplex. In contrast, the standard protocols for ExM generally involve removing ions to facilitate the swelling and uniform expansion of the gel. Therefore, the challenge in combining DNA-PAINT with ExM arises from the need to balance these requirements—metal ions for DNA-PAINT and ion-free conditions for optimal gel expansion. The absence of metal ions during the expansion process could significantly hinder DNA hybridization, leading to reduced binding speed and potential misfolding of DNA strands, while using saline buffers necessary for DNA hybridization could affect the expansion factor, potentially resulting in suboptimal sample expansion. Research is needed to identify the minimum concentration of metal ions that allows DNA-PAINT to function effectively without causing significant gel shrinkage. This optimization would be crucial for maintaining both the integrity of the expanded hydrogel and the efficiency of DNA hybridization.

The super-resolution MINFLUX approach has been recently developed to achieve high-resolution imaging with minimal phototoxicity and photobleaching. It is based on minimizing the fluorescence signal from a single molecule by precisely controlling the position of a donut-shaped excitation laser. This approach allows for the localization of individual molecules with high accuracy, enabling the reconstruction of high-resolution images. MINFLUX has been shown to achieve resolutions down to 1–2 nm, making it one of the highest resolution super-resolution techniques currently available.[154] Therefore, in theory, combining ExM with MINFLUX has the potential to achieve Angstrom-level resolution. However, despite this promising prospect, no work has been published to date on this combination. This lack of research may be attributed to the high cost and limited accessibility of MINFLUX technology. Additionally, at such high resolution, sample heterogeneity and distortion within the hydrogel might become more apparent, potentially leading to inaccurate data. In this context, tetragels might be more suitable for combining ExM with MINFLUX. However, the use of these novel gel chemistries is not yet widespread, due to limitations, such as the need for customized synthesis of the gel monomers. Another limitation again arises from the labeling strategy, as linkage errors become of increasing concern with higher resolutions and therefore a significant challenge at Angstrom-level resolution. A rapidly developing approach involving direct protein labeling with unnatural amino acids, which can be tagged with any fluorophore through click reaction may offer promising potential for combining ExM with MINFLUX.[155]

Thereby, further improvements in combining ExM with additional SRM techniques still require the development of new gel chemistries for improved structure preservation, enhanced labeling strategies to minimize or eliminate linkage errors, and fluorophores capable of withstanding expansion while maintaining their photophysical properties within the hydrogel environment.

Even at its current stage, the synergistic integration of ExM with SRM offers a powerful and versatile toolbox for nanoscale biological imaging. By leveraging the strengths of both methods, researchers can visualize cellular and tissue structures with unprecedented detail, opening the door to groundbreaking discoveries across fields ranging from neuroscience to pathology. As these techniques continue to mature and evolve, their potential applications in basic and translational research are set to expand, transforming our understanding of the complex processes that govern life at the nanoscale.

SUPPLEMENTARY MATERIAL

See the supplementary material for details as follows: Fig. 1 (workflow and pitfalls of combined methods) further illustrates various combined workflows and their challenges. A figure legend is embedded within the supplementary material. Table 1 (summary of expansion microscopy protocols) provides further information on different ExM protocols, including their maximal expansion factor and achieved lateral resolution.

ACKNOWLEDGMENTS

This work was supported by the following grants. (1) The Novo Nordisk Foundation (Young Investigator Award; NNF21OC0066381) to V.G.P.; (2) The German Research Foundation: CRC/1192 to V.G.P.; (3) German Federal Ministry of Education and Research: eMed Consortia Fibromap to V.G.P.; STOP-FSGS-01GM2202A to V.G.P.; (4) The Else-Kröner-Fresenius-Stiftung and the Eva Luise und Horst Köhler Stiftung (2019_KollegSE.04 RECORD) to D.K.; (5) The doctoral college "innovative Promotionsförderung im Bereich translationale Entzündungsforschung" (iPRIME) of the Else-Kröner-Fresenius Foundation to M.K.; (6) Intramural funding Clinician Scientist program to D.K.; (7) the Gulbenkian Foundation (Fundação Calouste Gulbenkian, H.S.H., D.A., M.D.R., and R.H.); (8) the European Research Council under the European Union's Horizon 2020 research and innovation program (Grant Agreement No. 101001332 to R.H.) and the European Commission through the Horizon Europe program (AI4LIFE project with Grant Agreement No. 101057970-AI4LIFE and RT-Super-ES project with Grant Agreement No. 101099654-RT-Super-ES to R.H.); funded by the European Union. Views and opinions expressed are, however, those of the authors only and do not necessarily reflect those of the European Union. Neither the European Union nor the granting authority can be held responsible for them. (9) the European Molecular Biology Organization (EMBO-2020-IG-4734 to R.H.); (10) the Fundação para a Ciência e Tecnologia, Portugal (FCT fellowship CEECIND/01480/2021 to H.S.H. and Associate Laboratory LS4FUTURE (LA/P/0087/2020,

DOI:10.54499/LA/P/0087/2020) to R.H.); (11) the Chan Zuckerberg Initiative Visual Proteomics Grant (vpi-0000000044 with https://doi.org/10.37921/743590vtudfp); and (12) Aarhus University Research Foundation, AUFF recruiting Grant No. AUFF-E-2022-7-13 to V.G.P and the Chan Zuckerberg Initiative Essential Open Source Software for Science (EOSS6-0000000260) to R.H. Schematics were created with BioRender.com.

AUTHOR DECLARATIONS

Conflict of Interest

The authors have no conflicts to disclose.

Author Contributions

Daria Aristova and Dominik Kylies contributed equally to this work as co-first authors, and Ricardo Henriques and Victor G. Puelles contributed equally to this work as co-senior and corresponding authors.

Daria Aristova: Conceptualization (equal); Formal analysis (equal); Methodology (equal); Visualization (equal); Writing – original draft (equal); Writing – review & editing (equal). **Dominik Kylies:** Conceptualization (equal); Formal analysis (equal); Methodology (equal); Visualization (equal); Writing – original draft (equal); Writing – review & editing (equal). **Mario Del Rosario:** Methodology (equal); Visualization (equal); Writing – review & editing (equal). **Hannah S. Heil:** Methodology (equal); Visualization (equal); Writing – review & editing (equal). **Maria Schwerk:** Methodology (equal); Writing – review & editing (equal). **Malte Kuehl:** Conceptualization (equal); Funding acquisition (equal); Methodology (equal); Visualization (equal); Writing – review & editing (equal). **Milagros N. Wong:** Methodology (equal); Supervision (equal); Writing – review & editing (equal). **Ricardo Henriques:** Conceptualization (equal); Funding acquisition (equal); Methodology (equal); Supervision (equal); Writing – original draft (equal); Writing – review & editing (equal). **Victor G. Puelles:** Conceptualization (equal); Funding acquisition (equal); Supervision (equal); Visualization (equal); Writing – original draft (equal); Writing – review & editing (equal).

DATA AVAILABILITY

Data sharing is not applicable to this article as no new data were created or analyzed in this study.

REFERENCES

[1]J. C. Stockert and A. Blazquez-Castro, *Fluorescence Microscopy in Life Sciences* (Bentham Science Publishers, 2017).
[2]S. J. Sahl, S. W. Hell, and S. Jakobs, "Fluorescence nanoscopy in cell biology," Nat. Rev. Mol. Cell Biol. **18**, 685–701 (2017).
[3]J. Montes, J. M. Peña, J. DeFelipe, O. Herreras, and A. Merchan-Perez, "The influence of synaptic size on AMPA receptor activation: A Monte Carlo model," PLoS One **10**, e0130924 (2015).
[4]F. Gabbiani and S. J. Cox, "Synaptic transmission and quantal release," in *Mathematics for Neuroscientists*, edited by F. Gabbiani and S. J. Cox (Academic Press, London, 2010), Chap. 12, pp. 175–191.
[5]L. Qin and J. M. Crawford, "Anatomy and cellular functions of the liver," in *Zakim and Boyer's Hepatology* (Elsevier, 2018), pp. 2–19.e4.
[6]F. Grahammer, C. Schell, and T. B. Huber, "The podocyte slit diaphragm—From a thin grey line to a complex signalling hub," Nat. Rev. Nephrol. **9**, 587–598 (2013).
[7]P. Sengupta *et al.*, "Probing protein heterogeneity in the plasma membrane using PALM and pair correlation analysis," Nat. Methods **8**, 969–975 (2011).
[8]K. Xu, G. Zhong, and X. Zhuang, "Actin, spectrin, and associated proteins form a periodic cytoskeletal structure in axons," Science **339**, 452–456 (2013).
[9]A. Honigmann *et al.*, "Phosphatidylinositol 4,5-bisphosphate clusters act as molecular beacons for vesicle recruitment," Nat. Struct. Mol. Biol. **20**, 679–686 (2013).
[10]D. Li *et al.*, "Extended-resolution structured illumination imaging of endocytic and cytoskeletal dynamics," Science **349**, aab3500 (2015).
[11]S. Galiani *et al.*, "Super-resolution microscopy reveals compartmentalization of peroxisomal membrane proteins," J. Biol. Chem. **291**, 16948–16962 (2016).
[12]J. C. Jennette and V. D. D'Agati, *Heptinstall's Pathology of the Kidney* (Wolters Kluwer, Philadelphia, 2024).
[13]A. J. Howie, *Handbook of Renal Biopsy Pathology* (Springer International Publishing, Cham, 2020).
[14]L. Schermelleh, R. Heintzmann, and H. Leonhardt, "A guide to super-resolution fluorescence microscopy," J. Cell Biol. **190**, 165–175 (2010).
[15]S. W. Hell and J. Wichmann, "Breaking the diffraction resolution limit by stimulated emission: Stimulated-emission-depletion fluorescence microscopy," Opt. Lett. **19**, 780 (1994).
[16]M. G. L. Gustafsson, "Surpassing the lateral resolution limit by a factor of two using structured illumination microscopy: Short communication," J. Microsc. **198**, 82–87 (2000).
[17]M. G. L. Gustafsson, "Nonlinear structured-illumination microscopy: Wide-field fluorescence imaging with theoretically unlimited resolution," Proc. Natl. Acad. Sci. U. S. A. **102**, 13081–13086 (2005).
[18]E. Betzig *et al.*, "Imaging intracellular fluorescent proteins at nanometer resolution," Science **313**, 1642–1645 (2006).
[19]M. J. Rust, M. Bates, and X. Zhuang, "Sub-diffraction-limit imaging by stochastic optical reconstruction microscopy (STORM)," Nat. Methods **3**, 793–796 (2006).
[20]S. T. Hess, T. P. K. Girirajan, and M. D. Mason, "Ultra-high resolution imaging by fluorescence photoactivation localization microscopy," Biophys. J. **91**, 4258–4272 (2006).
[21]M. Heilemann *et al.*, "Subdiffraction-resolution fluorescence imaging with conventional fluorescent probes," Angew. Chem. Int. Ed. **47**, 6172–6176 (2008).
[22]G. Giannone *et al.*, "Dynamic superresolution imaging of endogenous proteins on living cells at ultra-high density," Biophys. J. **99**, 1303–1310 (2010).
[23]R. Jungmann *et al.*, "Single-molecule kinetics and super-resolution microscopy by fluorescence imaging of transient binding on DNA origami," Nano Lett. **10**, 4756–4761 (2010).
[24]R. Jungmann *et al.*, "Multiplexed 3D cellular super-resolution imaging with DNA-PAINT and Exchange-PAINT," Nat. Methods **11**, 313–318 (2014).
[25]J. Huff, "The Airyscan detector from ZEISS: Confocal imaging with improved signal-to-noise ratio and super-resolution," Nat. Methods **12**, i–ii (2015).
[26]C. Bond, A. N. Santiago-Ruiz, Q. Tang, and M. Lakadamyali, "Technological advances in super-resolution microscopy to study cellular processes," Mol. Cell **82**, 315–332 (2022).
[27]A. Alva *et al.*, "Fluorescence fluctuation-based super-resolution microscopy: Basic concepts for an easy start," J. Microsc. **288**, 218–241 (2022).
[28]T. Dertinger, R. Colyer, G. Iyer, S. Weiss, and J. Enderlein, "Fast, background-free, 3D super-resolution optical fluctuation imaging (SOFI)," Proc. Natl. Acad. Sci. U. S. A. **106**, 22287–22292 (2009).
[29]N. Gustafsson *et al.*, "Fast live-cell conventional fluorophore nanoscopy with ImageJ through super-resolution radial fluctuations," Nat. Commun. **7**, 12471 (2016).
[30]R. Schmidt *et al.*, "MINFLUX nanometer-scale 3D imaging and microsecond-range tracking on a common fluorescence microscope," Nat. Commun. **12**, 1478 (2021).
[31]Y. Eilers, H. Ta, K. C. Gwosch, F. Balzarotti, and S. W. Hell, "MINFLUX monitors rapid molecular jumps with superior spatiotemporal resolution," Proc. Natl. Acad. Sci. U. S. A. **115**, 6117–6122 (2018).
[32]K. C. Gwosch *et al.*, "MINFLUX nanoscopy delivers 3D multicolor nanometer resolution in cells," Nat. Methods **17**, 217–224 (2020).
[33]M. Weber *et al.*, "MINSTED fluorescence localization and nanoscopy," Nat. Photonics **15**, 361–366 (2021).

[34]M. Weber *et al.*, "MINSTED nanoscopy enters the Ångström localization range," Nat. Biotechnol. **41**, 569–576 (2023).
[35]S. C. M. Reinhardt *et al.*, "Ångström-resolution fluorescence microscopy," Nature **617**, 711–716 (2023).
[36]F. Chen, P. W. Tillberg, and E. S. Boyden, "Expansion microscopy," Science **347**, 543–548 (2015).
[37]P. W. Tillberg *et al.*, "Protein-retention expansion microscopy of cells and tissues labeled using standard fluorescent proteins and antibodies," Nat. Biotechnol. **34**, 987–992 (2016).
[38]A. T. Wassie, Y. Zhao, and E. S. Boyden, "Expansion microscopy: Principles and uses in biological research," Nat. Methods **16**, 33–41 (2019).
[39]T. Ku *et al.*, "Multiplexed and scalable super-resolution imaging of three-dimensional protein localization in size-adjustable tissues," Nat. Biotechnol. **34**, 973–981 (2016).
[40]T. Ku *et al.*, "Elasticizing tissues for reversible shape transformation and accelerated molecular labeling," Nat. Methods **17**, 609–613 (2020).
[41]S. M. Asano *et al.*, "Expansion microscopy: Protocols for imaging proteins and RNA in cells and tissues," Curr. Protoc. Cell Biol. **80**, e56 (2018).
[42]D. N. Düring, M. D. Rocha, F. Dittrich, M. Gahr, and R. H. R. Hahnloser, "Expansion light sheet microscopy resolves subcellular structures in large portions of the songbird brain," Front. Neuroanat. **13**, 2 (2019).
[43]L. Pesce, P. Ricci, G. Sportelli, N. Belcari, and G. Sancataldo, "Expansion and light-sheet microscopy for nanoscale 3D imaging," Small Methods **8**, e2301715 (2024).
[44]L. Mascheroni *et al.*, "Combining sample expansion and light sheet microscopy for the volumetric imaging of virus-infected cells with super-resolution," Biomed. Opt. Express **11**, 5032 (2020).
[45]C.-H. Lu, C.-Y. Huang, X. Tian, P. Chen, and B.-C. Chen, "Large-scale expanded sample imaging with tiling lattice lightsheet microscopy," Int. J. Biochem. Cell Biol. **154**, 106340 (2023).
[46]J. H. Day *et al.*, "HiExM: High-throughput expansion microscopy enables scalable super-resolution imaging," bioRxiv (2023).
[47]M. Gao *et al.*, "Expansion stimulated emission depletion microscopy (ExSTED)," ACS Nano **12**, 4178–4185 (2018).
[48]F. U. Zwettler *et al.*, "Molecular resolution imaging by post-labeling expansion single-molecule localization microscopy (Ex-SMLM)," Nat. Commun. **11**, 3388 (2020).
[49]A. R. Halpern, G. C. M. Alas, T. J. Chozinski, A. R. Paredez, and J. C. Vaughan, "Hybrid structured illumination expansion microscopy reveals microbial cytoskeleton organization," ACS Nano **11**, 12677–12686 (2017).
[50]D. Kylies *et al.*, "Expansion-enhanced super-resolution radial fluctuations enable nanoscale molecular profiling of pathology specimens," Nat. Nanotechnol. **18**, 336–342 (2023).
[51]E. Abraham, J. Zhou, and Z. Liu, "Speckle structured illumination endoscopy with enhanced resolution at wide field of view and depth of field," Opto-Electron. Adv. **6**, 220163 (2023).
[52]X. Tian *et al.*, "Multi-prior physics-enhanced neural network enables pixel super-resolution and twin-image-free phase retrieval from single-shot hologram," Opto-Electron. Adv. **7**, 240060 (2024).
[53]Y. Xiao *et al.*, "Improved spatiotemporal resolution of anti-scattering super-resolution label-free microscopy via synthetic wave 3D metalens imaging," Opto-Electron. Sci. **2**, 230037 (2023).
[54]H. R. Ueda *et al.*, "Tissue clearing and its applications in neuroscience," Nat. Rev. Neurosci. **21**, 61–79 (2020).
[55]H. Hama *et al.*, "Scale: A chemical approach for fluorescence imaging and reconstruction of transparent mouse brain," Nat. Neurosci. **14**, 1481–1488 (2011).
[56]K. Chung *et al.*, "Structural and molecular interrogation of intact biological systems," Nature **497**, 332–337 (2013).
[57]E. A. Susaki *et al.*, "Whole-brain imaging with single-cell resolution using chemical cocktails and computational analysis," Cell **157**, 726–739 (2014).
[58]T. C. Murakami *et al.*, "A three-dimensional single-cell-resolution whole-brain atlas using CUBIC-X expansion microscopy and tissue clearing," Nat. Neurosci. **21**, 625–637 (2018).
[59]G. Wen, V. Leen, T. Rohand, M. Sauer, and J. Hofkens, "Current progress in expansion microscopy: Chemical strategies and applications," Chem. Rev. **123**, 3299–3323 (2023).
[60]I. Cho, J. Y. Seo, and J. Chang, "Expansion microscopy," J. Microsc. **271**, 123–128 (2018).
[61]S. Truckenbrodt, "Expansion microscopy: Super-resolution imaging with hydrogels," Anal. Chem. **95**, 3–32 (2023).
[62]T. J. Chozinski *et al.*, "Expansion microscopy with conventional antibodies and fluorescent proteins," Nat. Methods **13**, 485–488 (2016).
[63]Y. Zhao *et al.*, "Nanoscale imaging of clinical specimens using pathology-optimized expansion microscopy," Nat. Biotechnol. **35**, 757–764 (2017).
[64]F. Chen *et al.*, "Nanoscale imaging of RNA with expansion microscopy," Nat. Methods **13**, 679–684 (2016).
[65]S. Alon *et al.*, "Expansion sequencing: Spatially precise in situ transcriptomics in intact biological systems," Science **371**, eaax2656 (2021).
[66]J.-B. Chang *et al.*, "Iterative expansion microscopy," Nat. Methods **14**, 593–599 (2017).
[67]O. M'Saad and J. Bewersdorf, "Light microscopy of proteins in their ultrastructural context," Nat. Commun. **11**, 3850 (2020).
[68]V. Louvel *et al.*, "iU-ExM: Nanoscopy of organelles and tissues with iterative ultrastructure expansion microscopy," Nat. Commun. **14**, 7893 (2023).
[69]D. Gambarotto *et al.*, "Imaging cellular ultrastructures using expansion microscopy (U-ExM)," Nat. Methods **16**, 71–74 (2019).
[70]S. Truckenbrodt *et al.*, "X10 expansion microscopy enables 25-nm resolution on conventional microscopes," EMBO Rep. **19**, e45836 (2018).
[71]H. G. Damstra *et al.*, "Visualizing cellular and tissue ultrastructure using Ten-fold Robust Expansion Microscopy (TREx)," eLife **11**, e73775 (2022).
[72]A. Klimas *et al.*, "Magnify is a universal molecular anchoring strategy for expansion microscopy," Nat. Biotechnol. **41**, 858–869 (2023).
[73]D. M. Sherry and M. A. Stiles, "Improved fluorescent signal in expansion microscopy using fluorescent Fab fragment secondary antibodies," MethodsX **9**, 101796 (2022).
[74]M. Büttner *et al.*, "Challenges of using expansion microscopy for super-resolved imaging of cellular organelles," ChemBioChem **22**, 686–693 (2021).
[75]G. Wen, V. Leen, Y. Jia, T. Rohand, and J. Hofkens, "Improved dye survival in expansion microscopy through stabilizer-conjugated linkers," Chemistry **28**, e202202404 (2022).
[76]K. Min, I. Cho, M. Choi, and J.-B. Chang, "Multiplexed expansion microscopy of the brain through fluorophore screening," Methods **174**, 3–10 (2020).
[77]R. Gao, S. M. Asano, and E. S. Boyden, "Q&A: Expansion microscopy," BMC Biol. **15**, 50 (2017).
[78]M. Kang, J. Lee, S. Ko, and S. Shim, "Prelabeling expansion single-molecule localization microscopy with minimal linkage error," ChemBioChem **22**, 1396–1399 (2021).
[79]V. Hamel and P. Guichard, "Improving the resolution of fluorescence nanoscopy using post-expansion labeling microscopy," in *Methods in Cell Biology*, edited by P. Guichard and V. Hamel (Academic Press, 2021), Vol. 161, Chap. 14, pp. 297–315.
[80]S. M. Früh *et al.*, "Site-specifically-labeled antibodies for super-resolution microscopy reveal in situ linkage errors," ACS Nano **15**, 12161–12170 (2021).
[81]F. Liccardo *et al.*, "Precision localization of cellular proteins with fluorescent Fab-based probes," bioRxiv (2021).
[82]M. Erreni, T. Schorn, F. D'Autilia, and A. Doni, "Nanobodies as versatile tool for multiscale imaging modalities," Biomolecules **10**, 1695 (2020).
[83]L. Yao *et al.*, "Application of SNAP-tag in expansion super-resolution microscopy using DNA oligostrands," Front. Chem. **9**, 640519 (2021).
[84]E. Beghein and J. Gettemans, "Nanobody technology: A versatile toolkit for microscopic imaging, protein–protein interaction analysis, and protein function exploration," Front. Immunol. **8**, 771 (2017).
[85]R. S. Erdmann *et al.*, "Labeling strategies matter for super-resolution microscopy: A comparison between HaloTags and SNAP-tags," Cell Chem. Biol. **26**, 584–592.e6 (2019).
[86]R. Gao *et al.*, "A highly homogeneous polymer composed of tetrahedron-like monomers for high-isotropy expansion microscopy," Nat. Nanotechnol. **16**, 698–707 (2021).
[87]H. Lee, C.-C. Yu, E. S. Boyden, X. Zhuang, and P. Kosuri, "Tetra-gel enables superior accuracy in combined super-resolution imaging and expansion microscopy," Sci. Rep. **11**, 16944 (2021).
[88]J. Heine *et al.*, "Three dimensional live-cell STED microscopy at increased depth using a water immersion objective," Rev. Sci. Instrum. **89**, 053701 (2018).

[89]M. G. M. Velasco *et al.*, "3D super-resolution deep-tissue imaging in living mice," Optica **8**, 442 (2021).
[90]X. Chen *et al.*, "Superresolution structured illumination microscopy reconstruction algorithms: A review," Light: Sci. Appl. **12**, 172 (2023).
[91]J. Xu, H. Ma, and Y. Liu, "Stochastic optical reconstruction microscopy (STORM)," Curr. Protoc. Cytom. **81**, 12.46.1–12.46.27 (2017).
[92]C. K. Cahoon *et al.*, "Superresolution expansion microscopy reveals the three-dimensional organization of the Drosophila synaptonemal complex," Proc. Natl. Acad. Sci. U. S. A. **114**, E6857–E6866 (2017).
[93]B. Wang *et al.*, "Multicomposite super-resolution microscopy: Enhanced Airyscan resolution with radial fluctuation and sample expansions," J. Biophotonics **13**, e2419 (2020).
[94]A. H. Shaib *et al.*, "One-step nanoscale expansion microscopy reveals individual protein shapes," Nat. Biotechnol. (published online) (2024).
[95]T. C. Kunz, R. Götz, S. Gao, M. Sauer, and V. Kozjak-Pavlovic, "Using expansion microscopy to visualize and characterize the morphology of mitochondrial cristae," Front. Cell Dev. Biol. **8**, 617 (2020).
[96]D. Unnersjö-Jess *et al.*, "Confocal super-resolution imaging of the glomerular filtration barrier enabled by tissue expansion," Kidney Int. **93**, 1008–1013 (2018).
[97]D. Kim, T. Kim, J. Lee, and S. Shim, "Amplified expansion stimulated emission depletion microscopy," ChemBioChem **20**, 1260–1265 (2019).
[98]R. Li, X. Chen, Z. Lin, Y. Wang, and Y. Sun, "Expansion enhanced nanoscopy," Nanoscale **10**, 17552–17556 (2018).
[99]K. A. Saal *et al.*, "Heat denaturation enables multicolor X10-STED microscopy," Sci. Rep. **13**, 5366 (2023).
[100]H. Xu *et al.*, "Molecular organization of mammalian meiotic chromosome axis revealed by expansion STORM microscopy," Proc. Natl. Acad. Sci. U. S. A. **116**, 18423–18428 (2019).
[101]X. Shi *et al.*, "Label-retention expansion microscopy," J. Cell Biol. **220**, e202105067 (2021).
[102]I. Vojnovic, O. D. Caspari, M. A. Hoşkan, and U. Endesfelder, "Combining single-molecule and expansion microscopy in fission yeast to visualize protein structures at the nanostructural level," Open Biol. **14**, 230414 (2024).
[103]S. Culley, K. L. Tosheva, P. Matos Pereira, and R. Henriques, "SRRF: Universal live-cell super-resolution microscopy," Int. J. Biochem. Cell Biol. **101**, 74–79 (2018).
[104]T. Dertinger, R. Colyer, R. Vogel, J. Enderlein, and S. Weiss, "Achieving increased resolution and more pixels with Superresolution Optical Fluctuation Imaging (SOFI)," Opt. Express **18**, 18875 (2010).
[105]S. Cox *et al.*, "Bayesian localization microscopy reveals nanoscale podosome dynamics," Nat. Methods **9**, 195–200 (2012).
[106]F. Xu, M. Zhang, Z. Liu, P. Xu, and F. Zhang, "Bayesian localization microscopy based on intensity distribution of fluorophores," Protein Cell **6**, 211–220 (2015).
[107]I. Yahiatene, S. Hennig, M. Müller, and T. Huser, "Entropy-based super-resolution imaging (ESI): From disorder to fine detail," ACS Photonics **2**, 1049–1056 (2015).
[108]S. Geissbuehler *et al.*, "Mapping molecular statistics with balanced super-resolution optical fluctuation imaging (bSOFI)," Opt. Nanosc. **1**, 4 (2012).
[109]Y. S. Hu, X. Nan, P. Sengupta, J. Lippincott-Schwartz, and H. Cang, "Accelerating 3B single-molecule super-resolution microscopy with cloud computing," Nat. Methods **10**, 96–97 (2013).
[110]K. Agarwal and R. Macháň, "Multiple signal classification algorithm for super-resolution fluorescence microscopy," Nat. Commun. **7**, 13752 (2016).
[111]Y. Li *et al.*, "DLBI: Deep learning guided Bayesian inference for structure reconstruction of super-resolution fluorescence microscopy," Bioinformatics **34**, i284–i294 (2018).
[112]S. Culley *et al.*, "Quantitative mapping and minimization of super-resolution optical imaging artifacts," Nat. Methods **15**, 263–266 (2018).
[113]R. F. Laine *et al.*, "High-fidelity 3D live-cell nanoscopy through data-driven enhanced super-resolution radial fluctuation," Nat. Methods **20**, 1949–1956 (2023).
[114]J. D. Manton, "Answering some questions about structured illumination microscopy," Philos. Trans. R. Soc. A **380**, 20210109 (2022).
[115]N. Artelt *et al.*, "Comparative analysis of podocyte foot process morphology in three species by 3D super-resolution microscopy," Front. Med. **5**, 292 (2018).
[116]F. Siegerist *et al.*, "Structured illumination microscopy and automatized image processing as a rapid diagnostic tool for podocyte effacement," Sci. Rep. **7**, 11473 (2017).
[117]F. Siegerist, K. Endlich, and N. Endlich, "Novel microscopic techniques for podocyte research," Front. Endocrinol. **9**, 379 (2018).
[118]Y. Mo *et al.*, "Quantitative structured illumination microscopy via a physical model-based background filtering algorithm reveals actin dynamics," Nat. Commun. **14**, 3089 (2023).
[119]T. Zhao *et al.*, "Multi-color structured illumination microscopy for live cell imaging based on the enhanced image recombination transform algorithm," Biomed. Opt. Express **12**, 3474–3484 (2021).
[120]D. Karadaglić and T. Wilson, "Image formation in structured illumination wide-field fluorescence microscopy," Micron **39**, 808–818 (2008).
[121]M. A. A. Neil, R. Juškaitis, and T. Wilson, "Method of obtaining optical sectioning by using structured light in a conventional microscope," Opt. Lett. **22**, 1905 (1997).
[122]R. Heintzmann and T. Huser, "Super-resolution structured illumination microscopy," Chem. Rev. **117**, 13890–13908 (2017).
[123]M. T. M. Hannebelle *et al.*, "Open-source microscope add-on for structured illumination microscopy," Nat. Commun. **15**, 1550 (2024).
[124]M. Calvarese *et al.*, "Integrated optical device for Structured Illumination Microscopy," Opt. Express **30**, 30246 (2022).
[125]P. T. Brown, R. Kruithoff, G. J. Seedorf, and D. P. Shepherd, "Multicolor structured illumination microscopy and quantitative control of polychromatic light with a digital micromirror device," Biomed. Opt. Express **12**, 3700 (2021).
[126]X. Li *et al.*, "Three-dimensional structured illumination microscopy with enhanced axial resolution," Nat. Biotechnol. **41**, 1307–1319 (2023).
[127]L.-H. Yeh, L. Tian, and L. Waller, "Structured illumination microscopy with unknown patterns and a statistical prior," Biomed. Opt. Express **8**, 695 (2017).
[128]A. Lal, C. Shan, and P. Xi, "Structured illumination microscopy image reconstruction algorithm," IEEE J. Select. Top. Quantum Electron. **22**, 50–63 (2016).
[129]M. Bates, B. Huang, G. T. Dempsey, and X. Zhuang, "Multicolor super-resolution imaging with photo-switchable fluorescent probes," Science **317**, 1749–1753 (2007).
[130]A. Szymborska *et al.*, "Nuclear pore scaffold structure analyzed by super-resolution microscopy and particle averaging," Science **341**, 655–658 (2013).
[131]G. T. Dempsey, J. C. Vaughan, K. H. Chen, M. Bates, and X. Zhuang, "Evaluation of fluorophores for optimal performance in localization-based super-resolution imaging," Nat. Methods **8**, 1027–1036 (2011).
[132]G. Jacquemet, A. F. Carisey, H. Hamidi, R. Henriques, and C. Leterrier, "The cell biologist's guide to super-resolution microscopy," J. Cell Sci. **133**, jcs240713 (2020).
[133]T. A. Klar, E. Engel, and S. W. Hell, "Breaking Abbe's diffraction resolution limit in fluorescence microscopy with stimulated emission depletion beams of various shapes," Phys. Rev. E **64**, 066613 (2001).
[134]S. Liu, P. Hoess, and J. Ries, "Super-resolution microscopy for structural cell biology," Annu. Rev. Biophys. **51**, 301–326 (2022).
[135]G. Vicidomini, P. Bianchini, and A. Diaspro, "STED super-resolved microscopy," Nat. Methods **15**, 173–182 (2018).
[136]M. Hruska, N. Henderson, S. J. Le Marchand, H. Jafri, and M. B. Dalva, "Synaptic nanomodules underlie the organization and plasticity of spine synapses," Nat. Neurosci. **21**, 671–682 (2018).
[137]P. Ilgen *et al.*, "STED super-resolution microscopy of clinical paraffin-embedded human rectal cancer tissue," PLoS One **9**, e101563 (2014).
[138]H. Steffens, W. Wegner, and K. I. Willig, "In vivo STED microscopy: A roadmap to nanoscale imaging in the living mouse," Methods **174**, 42–48 (2020).
[139]F. Pan and W. Gan, "Two-photon imaging of dendritic spine development in the mouse cortex," Dev. Neurobiol. **68**, 771–778 (2008).
[140]S. Berning, K. I. Willig, H. Steffens, P. Dibaj, and S. W. Hell, "Nanoscopy in a living mouse brain," Science **335**, 551 (2012).
[141]M. J. T. Ter Veer, T. Pfeiffer, and U. V. Nägerl, "Two-photon STED microscopy for nanoscale imaging of neural morphology in vivo," in *Super-Resolution Microscopy*, edited by H. Erfle (Springer New York, New York, NY, 2017), Vol. 1663, pp. 45–64.
[142]C. A. Combs, D. L. Sackett, and J. R. Knutson, "A simple empirical algorithm for optimising depletion power and resolution for dye and system specific STED imaging," J. Microsc. **274**, 168–176 (2019).

[143]N. Kilian *et al.*, "Assessing photodamage in live-cell STED microscopy," Nat. Methods **15**, 755–756 (2018).
[144]M. P. Gordon, T. Ha, and P. R. Selvin, "Single-molecule high-resolution imaging with photobleaching," Proc. Natl. Acad. Sci. U. S. A. **101**, 6462–6465 (2004).
[145]X. Qu, D. Wu, L. Mets, and N. F. Scherer, "Nanometer-localized multiple single-molecule fluorescence microscopy," Proc. Natl. Acad. Sci. U. S. A. **101**, 11298–11303 (2004).
[146]A. Yildiz *et al.*, "Myosin V walks hand-over-hand: Single fluorophore imaging with 1.5-nm localization," Science **300**, 2061–2065 (2003).
[147]L. S. Churchman, Z. Ökten, R. S. Rock, J. F. Dawson, and J. A. Spudich, "Single molecule high-resolution colocalization of Cy3 and Cy5 attached to macromolecules measures intramolecular distances through time," Proc. Natl. Acad. Sci. U. S. A. **102**, 1419–1423 (2005).
[148]R. Thielhorn *et al.*, "Controlled grafting expansion microscopy," Angew. Chem. Int. Ed. **62**, e202302318 (2023).
[149]G. Wen *et al.*, "Evaluation of direct grafting strategies via trivalent anchoring for enabling lipid membrane and cytoskeleton staining in expansion microscopy," ACS Nano **14**, 7860–7867 (2020).
[150]J. Liu *et al.*, "Expansion microscopy with multifunctional polymer dots," Adv. Mater. **33**, 2007854 (2021).
[151]B. M. White, P. Kumar, A. N. Conwell, K. Wu, and J. M. Baskin, "Lipid expansion microscopy," J. Am. Chem. Soc. **144**, 18212–18217 (2022).
[152]J. Schnitzbauer, M. T. Strauss, T. Schlichthaerle, F. Schueder, and R. Jungmann, "Super-resolution microscopy with DNA-PAINT," Nat. Protoc. **12**, 1198–1228 (2017).
[153]D. Nieves, K. Gaus, and M. Baker, "DNA-based super-resolution microscopy: DNA-PAINT," Genes **9**, 621 (2018).
[154]F. Balzarotti *et al.*, "Nanometer resolution imaging and tracking of fluorescent molecules with minimal photon fluxes," Science **355**, 606–612 (2017).
[155]N. Elia, "Using unnatural amino acids to selectively label proteins for cellular imaging: A cell biologist viewpoint," FEBS J. **288**, 1107–1117 (2021).